AMERICAN SOCIETY FOR MICROBIOLOGY | Applied and Environmental Microbiology®

FOOD MICROBIOLOGY

Factors Required for Adhesion of *Salmonella enterica* Serovar Typhimurium to Corn Salad (*Valerianella locusta*)

Laura Elpers,[a] Juliane Kretzschmar,[a] Sean-Paul Nuccio,[b] Andreas J. Bäumler,[c] Michael Hensel[a,d]

[a]Abteilung Mikrobiologie, Universität Osnabrück, Osnabrück, Germany
[b]Department of Pediatrics, Division of Host-Microbe Systems and Therapeutics, University of California at San Diego, San Diego, California, USA
[c]Department of Medical Microbiology and Immunology, University of California at Davis, Davis, California, USA
[d]CellNanOs—Center for Cellular Nanoanalytics, Universität Osnabrück, Osnabrück, Germany

ABSTRACT *Salmonella enterica* is a foodborne pathogen often leading to gastroenteritis and is commonly acquired by consumption of contaminated food of animal origin. However, frequency of outbreaks linked to the consumption of fresh or minimally processed food of nonanimal origin is increasing. New infection routes of *S. enterica* by vegetables, fruits, nuts, and herbs have to be considered. This leads to special interest in *S. enterica* interactions with leafy products, e.g., salads, that are mainly consumed in a minimally processed form. The attachment of *S. enterica* to salad is a crucial step in contamination, but little is known about the bacterial factors required and mechanisms of adhesion. *S. enterica* possesses a complex set of adhesive structures whose functions are only partly understood. Potentially, *S. enterica* may deploy multiple adhesive strategies for adhering to various salad species and other vegetables. In this study, we systematically analyzed the contributions of the complete adhesiome, of lipopolysaccharide (LPS), and of flagellum-mediated motility of *S. enterica* serovar Typhimurium (STM) in adhesion to *Valerianella locusta* (corn salad). We deployed a reductionist, synthetic approach to identify factors involved in the surface binding of STM to leaves of corn salad, with particular regard to the expression of all known adhesive structures, using the Tet-on system. This work reveals the contribution of Saf fimbriae, type 1 secretion system-secreted BapA, an intact LPS, and flagellum-mediated motility of STM in adhesion to corn salad leaves.

IMPORTANCE Transmission of gastrointestinal pathogens by contaminated fresh produce is of increasing relevance to human health. However, the mechanisms of contamination of, persistence on, and transmission by fresh produce are poorly understood. We investigated the contributions of the various adhesive structures of STM to the initial event in transmission, i.e., binding to the plant surface. A reductionist system was used that allowed experimentally controlled surface expression of individual adhesive structures and analyses of the contribution to binding to leave surfaces of corn salad under laboratory conditions. The model system allowed the determination of the relative contributions of fimbrial and nonfimbrial adhesins, the type 3 secretion systems, the O antigen of lipopolysaccharide, the flagella, and chemotaxis of STM to binding to corn salad leaves. Based on these data, future work could reveal the mechanism of binding and the relevance of interaction under agricultural conditions.

KEYWORDS adhesiome, adhesion, fimbriae, fresh produce

Salmonella enterica is one of the main bacterial pathogens leading to foodborne illnesses and thousands of fatal cases worldwide (1). Depending on the serovar, *S. enterica* causes gastroenteritis (nontyphoidal serovar, e.g., Typhimurium) or typhoid

Citation Elpers L, Kretzschmar J, Nuccio S-P, Bäumler AJ, Hensel M. 2020. Factors required for adhesion of *Salmonella enterica* serovar Typhimurium to corn salad (*Valerianella locusta*). Appl Environ Microbiol 86:e02757-19. https://doi.org/10.1128/AEM.02757-19.

Editor Christopher A. Elkins, Centers for Disease Control and Prevention

Address correspondence to Michael Hensel, Michael.Hensel@uni-osnabrueck.de.

Received 27 November 2019
Accepted 4 February 2020
Accepted manuscript posted online 7 February 2020
Published 1 April 2020

fever (typhoidal serovars, e.g., Typhi and Paratyphi). Focus has historically been on infection routes of *Salmonella* by animal products, although in recent years, an increasing number of infections caused by fresh produce has been reported. In addition to pathogenic *Escherichia coli* (e.g., *E. coli* O157:H7) or *Listeria monocytogenes*, *S. enterica* is also involved in such plant-associated infections (2–4). Several outbreaks were associated with contaminated vegetables (e.g., tomatoes and salad), fruits (e.g., watermelons and berries), nuts, herbs (e.g., basil), and sprouts (5, 6). Fresh produce can be contaminated either through cultivation (contaminated irrigation water or fertilizer) or during handling and processing. *S. enterica* may adhere to leaves and roots, colonize the plant, and further internalize into the plant tissue (7, 8). Once inside the plant, *S. enterica* potentially can replicate and persist (9, 10). Endophytic *S. enterica* cannot be removed by surface washing, and bacteria will thus be ingested if food is consumed after minimal processing.

While the adhesion of *S. enterica* to mammalian cells has been investigated in great detail, far less is known about the mechanisms of interaction of *S. enterica* with plants. Investigation of adhesion to plant surfaces should allow better understanding of contamination and colonization of plant-based products by *S. enterica*. For the analyses of contamination of salads by *S. enterica*, the leafy part is of special interest, and the initial binding to salad leaves is a key event in the adhesion to and further colonization of salad. While surface contamination may occur by irrigation water or fecal shedding, a certain degree of adhesion is expected to maintain bacterium-plant association in the production process from "farm to fork."

In this study, we employed *S. enterica* serovar Typhimurium (STM) as a model pathogen causing gastroenteritis. STM possesses a large set of adhesive structures, including 12 chaperone-usher (CU) fimbriae, curli fimbriae assembled by the nucleation-precipitation pathway, two type 1 secretion system (T1SS)-secreted adhesins (BapA and SiiE), and three type 5 secretion system (T5SS)-secreted adhesins (MisL, ShdA, and SadA). Further, PagN and Rck are known outer membrane proteins (OMP) with putative adhesive features (reviewed in reference 11).

For most of the 12 CU fimbriae, little is known about their functional surface expression and binding properties (12). All operons encoding CU fimbriae consist of at least a fimbrial main subunit, a specific periplasmic chaperone, and a specific usher located in the outer membrane (13). The most prominent and best-studied fimbriae are Fim fimbriae encoded by the *fim* operon (*fimAICDHF*). Fim fimbriae are functionally expressed under static culture conditions and mediate binding to mannosylated proteins (14).

The *Salmonella* pathogenicity island 4 (SPI4) locus (*siiABCDEF*, *Salmonella* intestinal infection) encodes the giant adhesin SiiE, which is secreted to the bacterial surface by the T1SS SiiCDF (15). SiiE is known as the largest protein in STM, with 53 repetitive bacterial Ig (Big) domains and a molecular mass of 595 kDa. Moreover, SiiE exhibits binding specificity for glycostructures with terminal *N*-acetylglucosamine (GlcNAc) and 2,3-linked sialic acid (16). SiiE mediates the first contact of *Salmonella* with polarized epithelial cells of mammalian hosts (e.g., MDCK cells), enabling subsequent invasion mediated by the SPI1-encoded T3SS (here also referred to as SPI1-T3SS) and various effector proteins (17, 18). The *bap* operon (*bapABCD*, biofilm-associated protein) encodes a T1SS including BapB (outer membrane protein), BapC (ATPase), and BapD (membrane fusion protein) which is necessary for the secretion of the adhesin BapA to the bacterial surface. The T1SS-secreted adhesin BapA has a molecular mass of 386 kDa, contains 28 Big domains, and is involved in biofilm formation (19).

In addition, motility and chemotaxis mediated by flagellar rotation, as well as the adhesive effect of the lipopolysaccharide (LPS) layer, must be taken into consideration (11, 20). The specific binding properties of only a few adhesive structures of *S. enterica* are known, and thus, no educated guess can be made in regard to possible interactions with salad leaves. Several studies have investigated the adhesion of *S. enterica* serovars to various species of salad (9, 21–28), with a focus on individual adhesion factors. These studies succeeded in clarifying the first steps of colonization using wild-type (WT)

strains or mutant strains defective in single adhesion factors. Prior work revealed the involvement of flagella and motility, as well as further virulence-associated genes, in adhesion to salad. Further, the impact of different salad species was evaluated. Yet most studies on plant-pathogen interactions only tested differences in adhesion of one *Salmonella* isolate to various plant species or adhesion of various *Salmonella* serovars to one plant species (22, 23, 29).

A major obstacle for many analyses of *S. enterica* adhesion to vegetables was the lack of surface expression of functional adhesins in order to test their involvement. Indeed, only a minor proportion of adhesins is known to be expressed under laboratory conditions or defined environmental conditions. For example, global transcriptional analyses of STM under 22 defined culture conditions or stress exposure revealed significant transcriptional changes for only 3 of 20 adhesins (30; unpublished observation). It can thus be speculated that a subset of adhesins is expressed under environmental conditions outside of a warm-blooded host organism, although a systematic analysis of such expression is pending. To circumvent this limitation and to functionally express the entire adhesiome of STM, we recently devised a simple and robust approach based on the use of the P_{tetA} promoter and induction by the nonantibiotic tetracycline (Tet) derivative anhydrotetracycline (AHT) (31). In the present study, we deployed this technique to investigate the contributions of the various adhesive structures of STM to adhesion to the surface of corn salad leaves.

We have analyzed the impact of, to our knowledge, all adhesive structures of STM in adhesion to corn salad (*Valerianella locusta*). Moreover, we have found factors that are involved in the adhesion of STM to salad. With this knowledge, we are potentially able to devise defensive strategies in growing, harvesting, and processing fresh produce in order to decrease the incidence of *Salmonella* infections.

RESULTS

We deployed a reductionist, synthetic approach to identify factors that contribute to the surface binding of *Salmonella enterica* serovar Typhimurium (STM) to leaves of corn salad. As with all *S. enterica* serovars studied so far, STM possesses a complex adhesiome. We expressed the various operons or genes encoding adhesins ectopically under the control of a tetracycline-inducible promoter, as previously described (31). Strains harboring these Tet-on plasmids were subsequently tested for their contribution to adhesion to *Valerianella locusta* (corn salad). We selected corn salad as a salad species that can be easily cultured and infected under laboratory conditions, as well as being a representative fresh produce relevant to consumer health. Thus, corn salad served as a model organism in the national research consortium Plantinfect. The infection of corn salad grown under aseptic conditions by STM was performed as described schematically in Fig. S1 in the supplemental material.

Prior to analyzing the contribution of adhesive structures in adhesion to corn salad, we tested different deletion strains for their suitability as a negative control and as a host strain for heterologous expression. The laboratory conditions for native expression of only a few adhesins such as *fim* fimbriae are known. Moreover, the expression of a fimbrial adhesin can impact the expression of other systems, including other adhesins (32, 33). To avoid potential interference by these factors, we generated a strain lacking all 12 CU fimbriae (SR11 Δ12). Furthermore, a strain was generated lacking all known and putative adhesive structures in SR11 (Δ*fimAICDHF* Δ*stbABCD* Δ*sthABCDE* Δ*stfACDEFG* Δ*stiABCH* Δ*bcfABCDEFGH* Δ*safABCD* Δ*pefACD-orf5-orf6* Δ*stcABCD* Δ*stjEDCBA* Δ*stdAB* Δ*lpfABCDE*::KSAC Δ*misL* Δ*sadA* Δ*shdA* ΔSPI4 Δ*bapABCD* Δ*rck* Δ*pagN* Δ*csgBAC-DEFG*), which we termed SR11 Δ20. Under the assay conditions, both SR11 Δ12 and SR11 Δ20 showed the same level of adhesion to corn salad as WT SR11 (Fig. 1A). Therefore, we decided to use SR11 Δ12 in all further experiments to avoid any background expression of CU fimbriae during our assays. Furthermore, SR11 Δ12 strains with additional deletions of single adhesive structures showed no altered levels of adhesion compared to SR11 Δ12, except for deletion of SPI4 and of *bapABCD* (Fig. 1B). The deletion strain defective in SPI4, lacking SiiE, the corresponding T1SS, and acces-

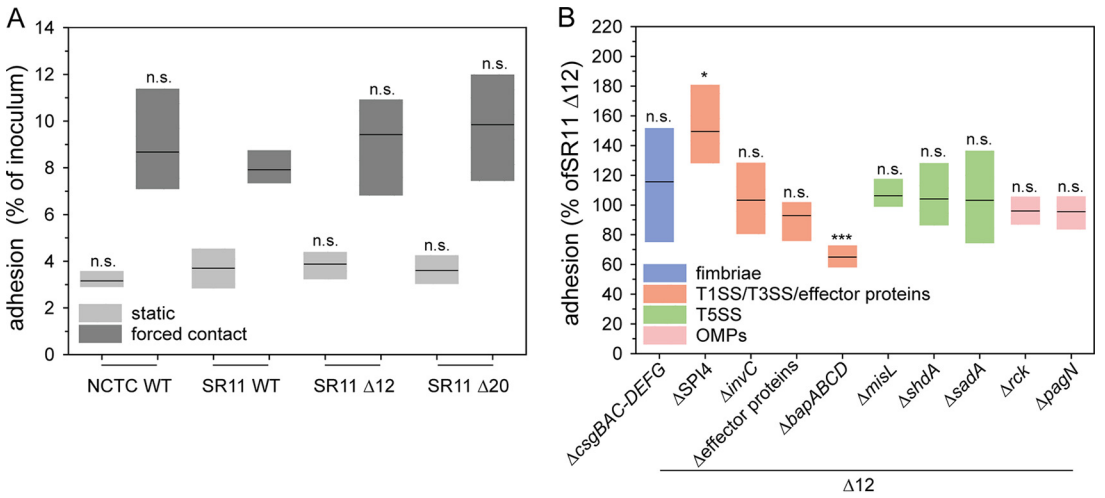

FIG 1 Comparison of *Salmonella* NCTC 12023 WT, SR11 WT, SR11 Δ12, and SR11 Δ20 and impact of deficits in genes encoding putative adhesive structures and effector proteins of SPI1-T3SS STM adhesion to corn salad. Corn salad grown under aseptic conditions was infected with STM NCTC 12023 WT, SR11 WT, SR11 Δ12, and SR11 Δ20 (A) and with SR11 Δ12 with various deletions in genes encoding putative adhesive structures and effector proteins of SPI1-T3SS (Δ*sopA* Δ*sopB* Δ*sopD* Δ*sopE2* Δ*sipA* [Δeffector proteins]) (B). Overnight cultures were diluted 1:31 in fresh LB, and bacteria were subcultured for 3.5 h and diluted in PBS for infection of corn salad. After infection for 1 h, corn salad segments were washed three times to remove nonadherent bacteria. For the quantification of adherent bacteria, corn salad leaf discs were homogenized in PBS containing 1% deoxycholate, and serial dilutions of homogenates and inoculum were plated onto MH agar plates for the quantification of CFU. Adhesion rates were determined by the ratio of CFU in inoculum and homogenate, and adherent bacteria normalized to SR11 Δ12 were set as 100% adhesion. Shown are the distributions of three biological replicates represented as box plots with medians. Statistical significances were calculated with Student's *t* test and are indicated as follows: n.s., not significant; *, $P < 0.05$; **, $P < 0.01$; and ***, $P < 0.001$.

sory proteins, showed increased adhesion (129% on average). The loss of adhesin BapA and its cognate T1SS BapBCD (Δ*bapABCD*) led to significantly decreased adhesion (65% on average). Of interest, BapA was not detected on the bacterial surface in 3.5-h subcultures of parental strain SR11 Δ12 (Fig. S2C and D).

Contribution of fimbrial adhesins to adhesion to corn salad. We analyzed adhesion to corn salad after P_{tetA}-induced expression of various CU fimbriae (Fig. 2A). The assay revealed distinct phenotypes of binding to corn salad. Expression of certain CU fimbriae by STM (Lpf, Bcf, Sth, Std, and Stj) resulted in adhesion levels similar to that of background strain SR11 Δ12, indicating that these adhesins do not have cognate

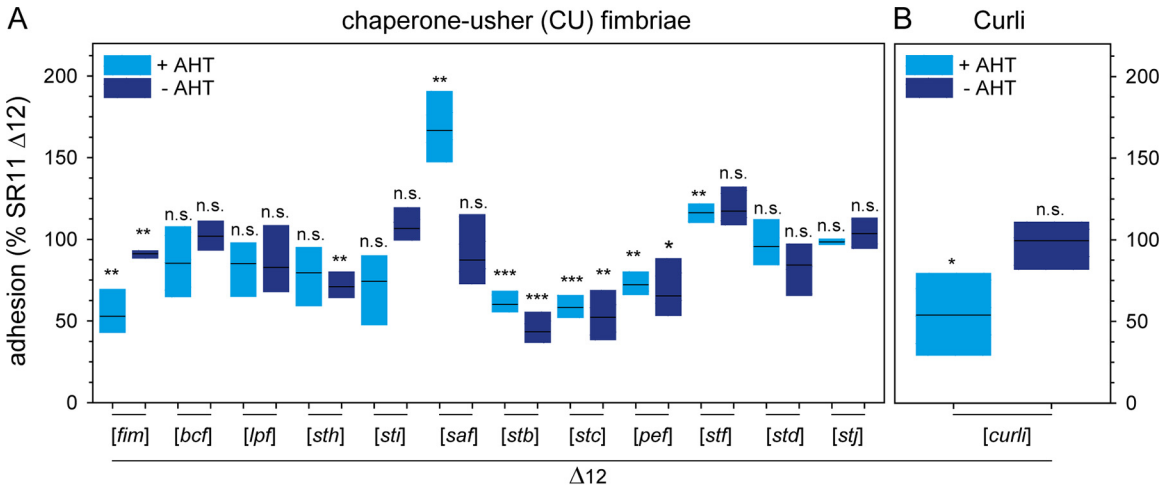

FIG 2 Impact of chaperone-usher fimbriae and curli fimbria expression on STM adhesion to corn salad. Sterile grown corn salad was infected with *S. enterica* serovar Typhimurium strain SR11 Δ12 with the expression of various chaperone-usher fimbriae (A) and the expression of curli fimbriae (B). Expression of fimbriae was induced with 10 ng/ml AHT for 3.5 h in subculture. The adhesion and statistical significances were determined as described in the legend to Fig. 1.

ligands on corn salad. Adhesion to corn salad was impaired after expression of Fim, Pef, Stc, and Stb fimbriae (53%, 72%, 58%, and 60% mean adhesion rates, respectively, compared to that of SR11 Δ12), while expression of Sti fimbriae resulted in slightly, but not significantly, decreased adhesion. In contrast, AHT-induced expression of Saf and Stf fimbriae led to increased adhesion (166% and 116% mean adhesion rates, respectively). A clear contribution of Saf fimbriae in adhesion to corn salad was confirmed by the noninduced control, exhibiting no altered adhesion level compared to that of background strain SR11 Δ12. Of note, a nonsignificant increase in adhesion was observed for Stf fimbriae in the absence of the inducer AHT, which was comparable to the case with AHT-induced samples. Consequently, a clear role for Stf fimbriae in adhesion of STM to corn salad cannot be ascribed.

Curli fimbriae are known to be involved in biofilm formation (34) and are encoded by two divergent operons, *csgBAC* and *csgDEFG*, with assembly occurring via the nucleation-precipitation pathway. AHT-induced expression of curli fimbriae showed a decreased adhesion to corn salad, whereas without AHT induction, no altered adhesion was observed (Fig. 2B).

Contribution of T1SS-secreted nonfimbrial adhesins to adhesion to corn salad. As generation of a vector for Tet-on expression of the *sii* operon turned out to be problematic, we deployed an alternative approach to control expression of the native *sii* operon. Enhanced surface expression of SiiE was achieved by AHT-induced overexpression of *hilD*, the central transcriptional activator of the SPI1/SPI4 regulon (35). We observed that increased amounts of SiiE on the bacterial surface led to decreased adhesion to corn salad (77% mean [Fig. 3A]) compared to that of SR11 Δ12 with native expression of SiiE in 3.5-h subcultures (Fig. S2A and B). Without induction by AHT and therefore with almost natural SiiE expression, no differences in adhesion from that of the background strain SR11 Δ12 were observed. Since the expression of the regulator *hilD* also influences the expression of the SPI1-encoded T3SS and its effector proteins, the plasmid carrying *hilD* was tested under the control of the Tet-on system in further SPI1 and SPI4 deletion mutants. Overexpression of *hilD* in an SPI4 deletion mutant led to a significantly decreased adhesion (53% on average), indicating that the SPI1-T3SS rather than SiiE itself interferes with the adhesion to corn salad. This was further confirmed by an increased adhesion rate of a strain lacking *invC* (ATPase subunit of SPI1-T3SS), and thereby the SPI1-T3SS, harboring a plasmid for *hilD* overexpression (153%). The deletion of *invC* alone, as well as deletion of the effector proteins SopA, SopB, SopD, SopE2, and SipA (Fig. 1B), did not alter adhesion, leading to the hypothesis that the SPI1-T3SS affects adhesion to corn salad.

AHT-induced expression of the *bap* operon led to increased adhesion to corn salad (124% mean [Fig. 3B]), whereas no significant differences were observed without AHT induction. To gain further insight into which structural features of BapA are essential for adhesion, we generated plasmids for Tet-on expression of *bapABCD* that encode BapA with deletions of Big domains to various extents. Synthesis and secretion of truncated forms of BapA were confirmed by flow cytometry (Fig. S2C and D) and indicated that deletion of Big1-28 and Big15-24 ablated the surface expression of BapA. This observation is in line with the adhesion assay results for strains expressing BapA harboring a deletion of Big1-28 or Big15-24, which showed no increased adhesion to corn salad. Thus, the loss of BapA surface expression resulted in adhesion levels comparable to that of SR11 Δ12. In contrast, truncated forms of BapA with deletion of only one Big domain, either Big1 or Big28, were detected on the bacterial surface by flow cytometry. Moreover, in adhesion assays, no increased adhesion was observed compared to that with wild-type BapA. Hence, the Big1 and Big28 domains might be relevant for proper binding to corn salad by BapA.

Contribution of autotransported adhesins to adhesion to corn salad. STM expresses three autotransported adhesins: MisL, ShdA, and SadA. MisL and ShdA are monomeric adhesins, whereas SadA belongs to the class of trimeric adhesins. Previous studies have shown that MisL and ShdA are involved in binding to fibronectin, which impacts intestinal infection of mice (36, 37). SadA is possibly involved in adhesion to

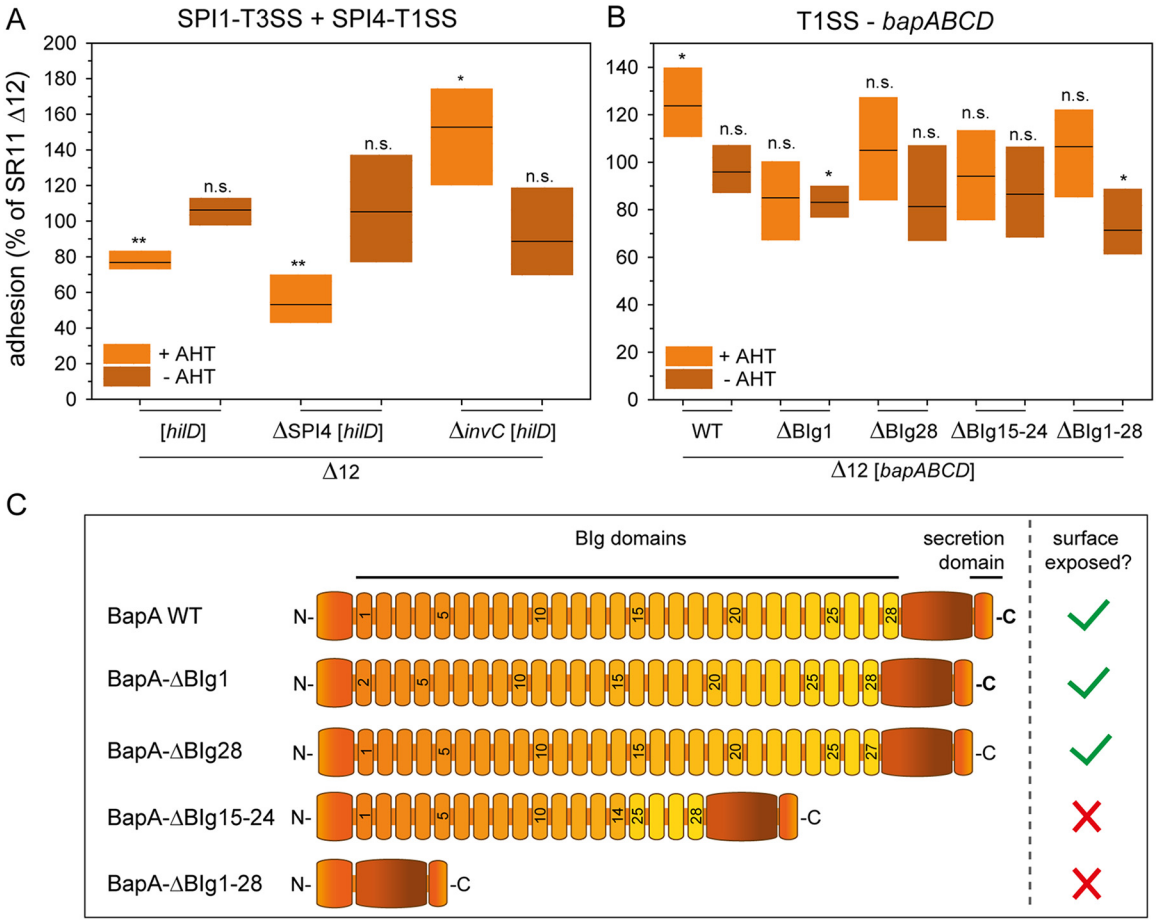

FIG 3 Impact of T1SS-secreted adhesins and *hilD* expression on STM adhesion to corn salad. Corn salad grown under aseptic conditions was infected with STM strain SR11 Δ12 with the overexpression of the regulator *hilD* for analysis of the SPI4-encoded, T1SS-secreted adhesin SiiE and the SPI1-encoded T3SS (A). In addition, SR11 Δ12 expressing AHT-induced, T1SS-secreted wild-type adhesin BapA or the indicated BapA truncation mutants were tested (B). The adhesion and the statistical significances were determined as described in the legend to Fig. 1. (C) Schematic overview of truncated BapA forms used in adhesion assays.

CaCo2 cells, as well as in biofilm formation, but only in a strain background with altered LPS structure (38). AHT-induced expression of *misL* did not alter adhesion to corn salad (Fig. 4A). In contrast, the AHT-induced expression of *shdA* led to a decreased average adhesion of 67%, whereas the noninduced strain displayed no changes in adhesion. The AHT-induced expression of *sadA* and its chaperone *sadB* led to a slight, but nonsignificantly, decreased adhesion (79% mean). Although we observed significantly higher adhesion (158% mean) without AHT induction, SadA surface expression was not detected by flow cytometry in noninduced samples (Fig. S2E and F).

Contribution of OMP adhesins to adhesion to corn salad. The OMPs Rck and PagN are adhesive structures, and an involvement in SPI1-T3SS-independent invasion of epithelial cells has been reported (39, 40). AHT-induced expression of *rck* led to a significantly decreased adhesion to corn salad (65% mean), although even the noninduced sample exhibited decreased adhesion (65% mean [Fig. 4B]). In a previous study, Western blot analyses confirmed the absence of expression of Rck in noninduced cultures (31). The AHT-induced expression of PagN exhibited significantly reduced adhesion (59% on average), whereas the noninduced samples showed no altered adhesion level.

Contribution of flagellar filaments and motility to adhesion to corn salad. The effect of flagella and motility on infection of various plants has been previously investigated for *Salmonella* and other pathogenic bacteria (25, 41, 42). In this study, we

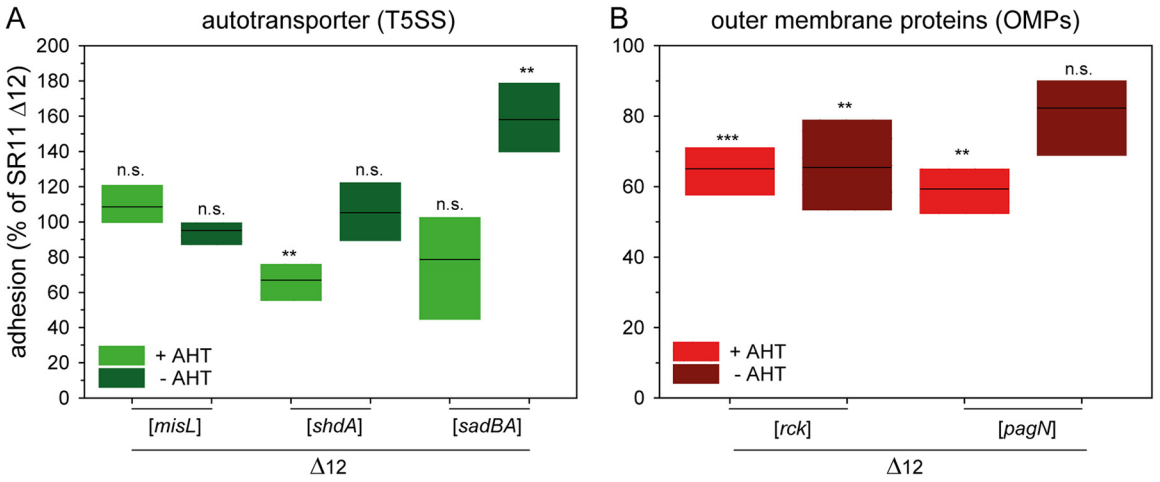

FIG 4 Impact of T5SS-secreted adhesins and of outer membrane proteins on STM adhesion to corn salad. (A) Corn salad grown under aseptic conditions was infected with STM strain SR11 Δ12 expressing the different T5SS-secreted adhesins MisL, ShdA, and SadA induced by AHT. (B) For the analysis of outer membrane proteins, SR11 Δ12 expressing *rck* and *pagN* by induction of AHT was used. The adhesion and the statistical significances were determined as described in the legend to Fig. 1.

demonstrated the binding properties and the contribution of motility in adhesion to corn salad using four distinct deletion strains. The deletion of *fliC* and *fljB*, resulting in the loss of the flagellar filament, yielded a decreased adhesion (50% mean) which could not be restored to background strain level by centrifugation (Fig. 5A). This effect may thus be due to an adhesive feature of the flagellar filament or due to flagellum-mediated motility promoting contact with corn salad surfaces. To dissect the contribution of flagella, a *motAB* mutant strain was employed; such strains still produce a flagellar filament, but they are unable to energize the flagellar motor and are thus nonmotile. The Δ*motAB* strain showed decreased adhesion for static and centrifuged samples (67% and 73% means, respectively). Thus, the presence of flagella without motility does not enable *Salmonella* to bind to corn salad. To gain further insight into how motility contributes to adhesion to corn salad, we deployed mutant strains with defective *cheY*, resulting in a strong bias toward smooth swimming, or defective *cheZ*, resulting in a strong bias for tumbling (Fig. 5C). The Δ*cheY* strain showed a decreased adhesion (71% mean) after centrifugation, whereas the deletion of *cheZ* led to a decreased adhesion which did not represent a statistically significant difference in static and centrifuged samples. We conclude that proper flagellum-mediated motility contributes to adhesion to corn salad surfaces and that this effect is not caused solely by the interaction of the flagellar filament with the leaf surface.

Contribution of O antigen to adhesion to corn salad. The major constituent of the Gram-negative cell surface is LPS. In addition to stabilization of the cell envelope and protection against various environmental factors, LPS increases the negative charge of the cell envelope, and a putative adhesive role has been reported (43). To analyze the impact of LPS in adhesion to corn salad, we used mutant strains lacking various genes involved in the biosynthesis of the O antigen of LPS. WT *Salmonella* displays a heterogeneous distribution of long-chain O antigen (L-OAg) and very-long-chain O antigen (VL-OAg). Deletion of *wzz* results in the homogenous distribution of VL-OAg, deletion of *fepE* results in the homogenous distribution of L-OAg, and a strain lacking both genes (*wzz fepE*) can only synthesize short O antigen (S-OAg) (Fig. 5D). The deletion of *rfaL* leads to the lack of O antigen, resulting in LPS being restricted to the core oligosaccharides.

In this study, the deletion of *wzz* and *wzz fepE* led to a decreased adhesion (49% and 52%, respectively) in static samples (Fig. 5B). The deletion of *rfaL* yielded a decreased adhesion (82% mean) which did not represent a statistically significant difference. The strain lacking *fepE* showed no altered adhesion. These data suggest that the presence

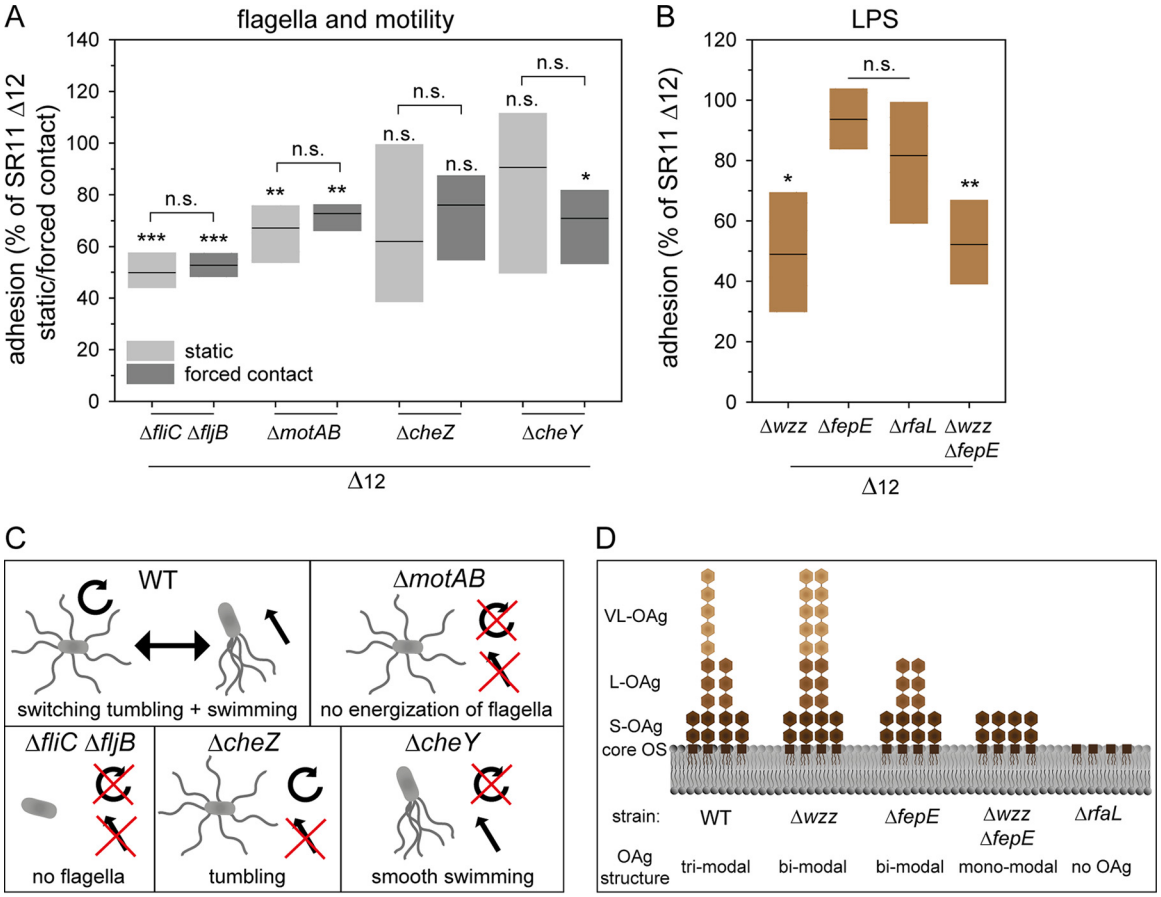

FIG 5 Impact of defect in motility and flagellar assembly and deletion of LPS structure on STM adhesion to corn salad. Corn salad grown under aseptic conditions was infected with STM strain SR11 Δ12 with deletion of various motility and flagellum-associated genes (A) and deletion of LPS structure-related genes (B). The infection took place either under static conditions or after centrifugation at 500 × *g* for 5 min to compensate effects of mutations in motility genes. For deletion of genes involved in O-antigen (OAg) biosynthesis, only static samples are shown. The adhesion and the statistical significances were determined as described in the legend to Fig. 1. Models of the resulting phenotype depending on the different deletions in motility flagellar assembly and LPS structure are depicted in panels C and D. Panel D is based on reference 46. OS, oligosaccharide.

of only VL-OAg or only S-OAg impairs binding to corn salad, and as a consequence, the L-OAg has to be present. The observation that the *rfaL* deletion, resulting in a lack of O antigen, led to no significant decrease in adhesion could be explained by binding of the core oligosaccharide to corn salad.

DISCUSSION

To address the question of which factors of *S. enterica* are involved in adhesion to plant surfaces, we deployed a reductionist, synthetic approach. This allowed controlled surface expression of specific adhesive structures of STM, one at a time. The various adhesive structures were tested for their impact on adhesion to corn salad leaves as a representative fresh produce, and the results of this study are summarized in Fig. 6.

Several prior studies showed that absence of the flagellar filament had an influence on adhesion to various plants. Whereas Berger et al. (21) reported a decreased adhesion to basil leaves for a Δ*fliC* Δ*fljB* strain of *S. enterica* serovar Senftenberg, Iniguez et al. (44) revealed an enhanced colonization of *Arabidopsis thaliana* roots for a Δ*fliC* Δ*fljB* mutant of STM. Thus, there has to be a clear difference in the role of flagella between colonization of the rhizosphere and of the phyllosphere. For the colonization of roots, the presence of flagella is apparently obstructive, due to pathogen-associated molecular pattern (PAMP)-triggered immunity of Flg22 by receptor kinase FLS2 recognition in *A. thaliana* (44, 45). For the first contact of *S. enterica* and other pathogenic bacteria

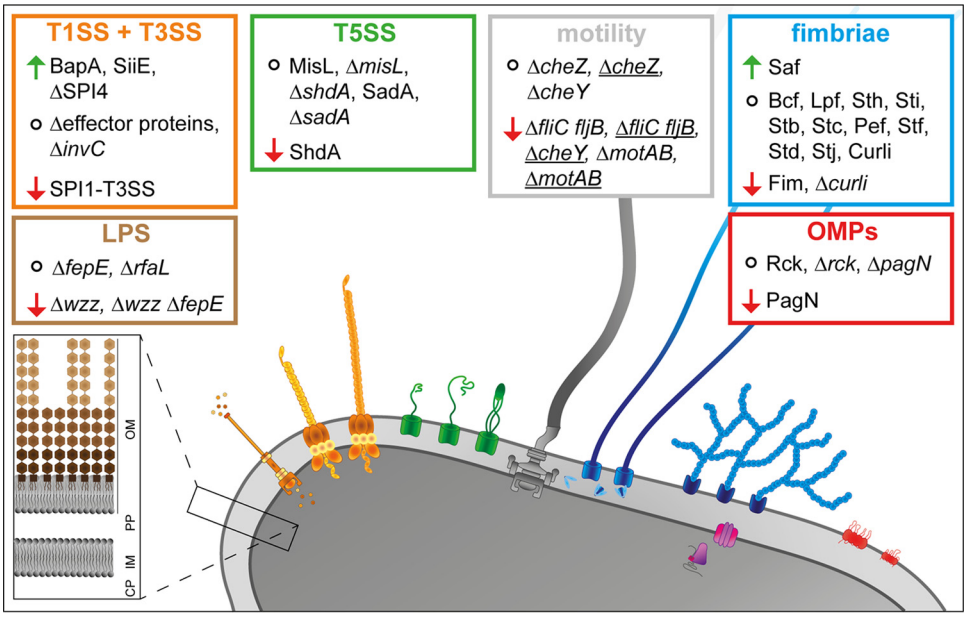

FIG 6 Overview of the impact of the analyzed factors of STM in adhesion to corn salad. The absence of underlining indicates static samples, and underlining indicates centrifuged samples. Arrows indicate increased or decreased adhesion, and circles indicate that adhesion was not altered. OM, outer membrane; PP, periplasm; IM, inner membrane; CP, cytoplasm.

with leaf surfaces, the presence of flagella is of crucial importance. To investigate the possible binding of flagellar filaments, Rossez et al. (42) purified the flagellar filament of pathogenic enterohemorrhagic *E. coli* (EHEC) O157:H7 Sakai, enteropathogenic *E. coli* (EPEC) O127:H6, and nonpathogenic *E. coli* K-12 with flagellar serotype H48. They showed that the binding of purified flagellar filaments to multiple plant lipid species (SQDG [sulfated glycolipid], phosphatidylcholine, phosphatidylglycerol, phosphatidylinositol, and phosphatidylethanolamine) results in the assumption of an ionic adhesion by binding to sulfated and phosphorylated plant plasma membrane lipids with negative charge. In addition, *E. coli* strain TUV93-0 Δ*fliC* showed a decreased adhesion to *Arabidopsis* leaves which could be reversed through complementation by all three flagellar serotypes (42). Possibly, the ionic adhesion of flagellar filaments represents a conserved mechanism for adhesion to plant leaves among Gram-negative bacteria.

Despite analyses of flagellar filament involvement in adhesion to various plant organs, less is known about the impact of motility. Kroupitski et al. (25) showed that deletion of *cheY* in STM had no consequences for attachment to iceberg lettuce leaves, whereas the internalization of STM was affected. The authors hypothesize that STM cannot reach stomata due to the lack of directed motility. Directed motility conceivably enables STM to sense sucrose near stomata, facilitating internalization. Thus, internalization was impaired during an experiment performed in the dark with fusicoccin-treated leaves, leading to constitutively opened stomata without producing sucrose by photosynthesis (25). In this study, we detected decreased adhesion levels for strains lacking flagellar filaments (Δ*fliC* Δ*fljB*) or the energization of flagellar rotation (Δ*motAB*), under conditions of either natural contact or forced contact. We therefore conclude that flagellar filaments are needed for not only adhesion to corn salad leaves but also motility. We observed only moderate effects on adhesion to corn salad leaves in the absence of either clockwise (CW) or counterclockwise (CCW) rotation, leading to the assumption that the flagellar filament and energization of at least CW or CCW rotation are necessary for binding to corn salad leaves. However, bacteria might utilize directed motility for accumulation near stomata and/or colonization of plant leaves.

The LPS layer of STM and other pathogenic bacteria was often examined with a focus on adhesion to, and invasion of, mammalian cells and for the impact on

inflammatory responses. The impact of LPS on adhesion to plant leaves, roots, and fruits remained unclear. Mutant strains of STM lacking very long OAg, or long and very long OAg, revealed higher levels of invasion of HeLa and MDCK cells, whereas deletion of the whole OAg even led to a highly increased adhesion to both cell lines. Despite this virulence advantage for STM, immune escape was reduced due to higher effector protein translocation (46). In contrast to an enhanced adhesion to mammalian cells due to an altered LPS structure of STM, we found that an altered LPS structure resulted in decreased adhesion to corn salad leaves. Our findings are in line with a study by Jang and Matthews (47) revealing that a truncated OAg in pathogenic *E. coli* O157:H7 decreases the ability to survive and persist on *Arabidopsis* plants as well as on romaine lettuce. In addition to pathogenic bacteria, an intact LPS structure is also important in nonpathogenic bacteria, like *Herbaspirillum seropedicae*, which acts as a symbiont for many agriculturally important plants. An altered LPS structure in *H. seropedicae* led to decreased attachment to maize root surfaces and to further endophytic colonization (48). These results were also observed for WT *H. seropedicae* when LPS, *N*-acetylglucosamine, or glucosamine was added to act as a competitor for binding sites. Here we show the importance of STM LPS in adhesion to leaf surfaces.

Regardless of LPS and motility of STM, adhesion was increased by expression of different adhesins. Saf fimbriae (*Salmonella* atypical fimbriae) were the only fimbriae of the CU pathway found in this study to enhance STM adhesion to corn salad leaves. Salih et al. (49) revealed by electron microscopy the highly flexible linear structure of Saf fimbriae belonging to FG-loop long (FGL) fimbriae. In contrast to rigid, rod-shaped FG-loop short (FGS) fimbriae, which exhibit various subunits with a distal adhesive tip, FG-loop long fimbriae often display only two subunits (50). Therefore, the adhesive unit is likely formed by the most numerous subunits. Thus, FGL fimbriae, like Saf fimbriae, might bind to a high number of receptors or ligands (49). Nevertheless, binding properties of Saf fimbriae are unknown. Until now, Saf fimbriae were reported to be involved in biofilm formation and in binding to porcine intestine IPEC-J2 cells (51). In addition, expression of Saf fimbriae was observed only during infection of murine spleen (52). Genes of the *saf* operon are often pseudogenes in host-restricted *S. enterica* serovars (Typhi, Paratyphi, and Gallinarum) (20), indicating their potential contribution in STM to dispersal by farm animals and newly investigated environmental routes, e.g., leafy plants and other vegetables. To gain further insight into the contribution of Saf fimbria adhesion of STM to plants, binding properties of Saf fimbriae have to be investigated, for example, by glycan arrays (42, 53) or by a detailed mutagenesis of potential binding domains.

In this study, we showed that T1SS-secreted adhesins SiiE and BapA both contribute to adhesion to corn salad leaves. While SiiE involvement in adhesion to mammalian polarized epithelial cells by binding GlcNAc and sialic acid is well understood (16, 17), a potential role for SiiE in adhesion to plant surfaces is less likely. The tight control of expression of the SPI1/SPI4 regulon by host cell factors would exclude surface expression of SiiE under environmental conditions. A contribution to adhesion was shown for T1SS-secreted adhesin BapA, and BapA contributes to biofilm formation (54), especially for formation of pellicles on the air-liquid interface (19). Furthermore, deletion of BapA led to a decreased mortality in mouse infection. Our data obtained after 1 h of infection excluded the possibility of biofilm formation by BapA-expressing STM on corn salad leaves. However, specific binding properties are unknown. To gain further insight into properties of binding of BapA to corn salad leaves, various truncated forms of BapA were tested. Truncated forms of BapA lacking one Big domain were surface expressed and showed no autoaggregation. Deletion of one or more Big domains reduced BapA-dependent adhesion. Thus, we propose a diminished adhesion to corn salad leaves by a shortened BapA. This hypothesis is further supported by the fact that deletion of Big1, possibly never reaching out of the OAg layer in WT BapA, results in a phenotype similar to that with deletion of Big28, possibly reaching out of LPS layer first in WT BapA. Further characterization of BapA binding to corn salad leaves is necessary,

including investigating the importance of proper folding of BapA in the presence of Ca^{2+} (55) and specific binding properties.

This study showed that adhesion of STM to corn salad leaves depends on an intact LPS layer and on flagellum-mediated motility. Further, we revealed the involvement in adhesion to corn salad leaves by expression of CU pathway-assembled Saf fimbriae, T1SS-secreted SiiE, and T1SS-secreted BapA. To gain further insight into adhesion of STM to salad, additional salad species should be investigated to assess if the detected contributing structures are also involved in adhesion to other salad species, or even to leafy plants in general. Moreover, a transcriptomic and proteomic analysis of the involved adhesins could further elucidate environmental conditions or conditions during colonization of plants. We used a synthetic system with controlled expression of one adhesive factor at a time. Whether the adhesive factors determined in this study are also expressed and functional under conditions of natural contamination of plants has to be investigated in further studies.

In summary, this work contributed to identification of STM adhesive factors required for adhesion to plants. To take these studies to a global context and to study the pathogen-plant interaction under field-like conditions, a more complex experimental setting is needed.

MATERIALS AND METHODS

Bacterial strains and culture conditions. Bacterial strains used in this study are listed in Table 1. Unless otherwise mentioned, bacteria were routinely grown aerobically in LB (lysogeny broth) medium or on LB agar containing antibiotics if required for selection of specific markers. Carbenicillin (Carb), nalidixic acid (Nal), or kanamycin (Km) was used to a final concentration of 50 μg/ml if required for the selection of phenotypes or maintenance of plasmids. Chloramphenicol (Cm) was used at 30 μg/ml. When needed for cloning purposes, 5-bromo-4-chloro-3-indolyl-β-D-galactopyranoside (X-Gal) was added to LB agar at 20 μg/ml. For the induction of the Tet-on system, anhydrotetracycline (AHT) was used at a final concentration of 10 ng/ml or 100 ng/ml.

Construction of Δ12 strain with a deletion of the chaperone-usher fimbrial gene cluster. Strains are listed in Table 1, plasmids (and the extent of each fimbrial gene cluster deletion) in Table 2, and oligonucleotides in Table 3. For cloning, *E. coli* DH5α was used as a host for pCR2.1 and pBluescriptII-derived plasmids, whereas *E. coli* CC118 λ*pir* was used as a host for pRDH10-derived plasmids. To generate the unmarked Δ*lpf*, Δ*pef*, Δ*saf*, Δ*stc*, and Δ*stj* allelic-exchange-mediated deletion constructs, upstream and downstream regions flanking the respective gene cluster to be deleted were amplified from the genome of *S. enterica* serovar Typhimurium LT2 by PCR with primers containing (i) restriction sites that enable ligation of the flanking regions together at their proximal ends, as well as that enable future introduction of an antibiotic resistance cassette, and (ii) restriction sites to enable subcloning of the deletion construct into the sucrose-counterselectable pRDH10 suicide vector. With the exception of the Δ*lpf* construct, flanking region PCR products were gel purified (QIAEX II kit; Qiagen), digested with XbaI (New England BioLabs [NEB]), ligated with T4 DNA ligase (NEB), and then PCR amplified by utilizing the distal primer of each respective flanking region's primer pair. Products were then cloned into pCR2.1 via the TOPO TA kit (Invitrogen), and correct inserts were confirmed by Sanger sequencing (SeqWright). For the Δ*lpf* construct, each flanking region was PCR amplified, gel purified, cloned separately into pCR2.1, and then confirmed by sequencing. The flanking regions were then joined together by sequential subcloning into pBluescriptII KS+. The unmarked Δ*lpf*, Δ*pef*, Δ*saf*, Δ*stc*, and Δ*stj* constructs were then subcloned into pRDH10. To generate the unmarked Δ*std* and Δ*sti* constructs in pRDH10, the Km resistance cassette was removed from pEW5 and pEW13, respectively, by restriction digestion, and then the vectors were gel purified and religated. As pSF2 (pRDH10 Δ*fim*) did not confer appreciable sucrose sensitivity to strains harboring it, the Δ*fim* construct was subcloned into another site in pRDH10: following EcoRI digestion of pSF2, the Δ*fim* construct was gel purified, blunted (QuickBlunt; NEB), and subcloned into the blunted BamHI site of pRDH10, yielding pSPN22. To generate Km-marked deletion constructs, the KSAC cassette of pBS34 was excised with XbaI or PstI as relevant, gel purified, and then subcloned between the flanking regions of the Δ*lpf*, Δ*pef*, Δ*saf*, Δ*stc*, and Δ*stj* constructs in their respective pRDH10-based vectors. To enable their conjugation, all unmarked and KSAC-marked pRDH10-based fimbrial gene cluster deletion vectors were electroporated into *E. coli* S17-1 λ*pir*.

S. Typhimurium IR715-derived strains harboring a single, KSAC-marked deletion of *lpf*, *pef*, *saf*, *stc*, or *stj* (e.g., SPN195 = IR715 Δ*saf*::KSAC) were generated by conjugation through mating of the respective S17-1 λ*pir* pRDH10(Δ::KSAC) strain with IR715. Transconjugants were selected for on LB-Km-Nal agar, and those resulting from a double-crossover event were screened for by sensitivity to Cm and then validated by PCR using primer pairs to confirm that KSAC was located in the correct genomic context, as well as by being negative for PCR amplification of the relevant fimbrial gene cluster's predicted major subunit gene.

Eleven (*bcf*, *fim*, *pef*, *saf*, *stb*, *stc*, *std*, *stf*, *sth*, *sti*, and *stj*) of the 12 KSAC-marked fimbrial gene cluster deletion strains were then converted to unmarked deletion strains (e.g., SPN230 = IR715 Δ*saf*) by mating the respective S17-1 λ*pir* pRDH10(Δ) and IR715 Δ::KSAC strains. Transconjugants with pRDH10(Δ)

TABLE 1 Bacterial strains used in this study

Strain	Relevant characteristics	Reference or source
E. coli CC118 λpir	Cloning strain for λpir-dependent plasmids	60
E. coli DH5α MCR	Cloning strain	61
E. coli NEB5α	Cloning strain	New England Biolabs
E. coli S17-1 *λpir*	Mobilization strain for plasmids containing $oriV_{R6K}$ and mob_{RP4}	62
S. Typhimurium IR715	*Salmonella enterica* serovar Typhimurium ATCC 14028s, spontaneous Nal^r	63
S. Typhimurium LT2	Wild type	64
S. Typhimurium NCTC12023	Wild type	NCTC
S. Typhimurium SR11	Wild type	65
AJB754	IR715 Δ*stiABCH*::KSAC	66
AJB786	IR715 Δ*stbABCD*::KSAC	66
EHW1	IR715 Δ*bcfABCDEFGH*::KSAC	66
EHW2	IR715 Δ*fimAICDHF*::KSAC	66
EHW3	IR715 Δ*stfACDEFG*::KSAC	66
EHW11	IR715 Δ*stdAB*::KSAC	66
SF22	IR715 Δ*sthABCDE*::KSAC	66
SPN191	IR715 Δ*bcfABCDEFGH*	This study
SPN192	IR715 Δ*fimAICDHF*	This study
SPN193	IR715 Δ*lpfABCDE*::KSAC	This study
SPN195	IR715 Δ*safABCD*::KSAC	This study
SPN196	IR715 Δ*stbABCD*	This study
SPN198	IR715 Δ*stdAB*	This study
SPN199	IR715 Δ*stfACDEFG*	This study
SPN200	IR715 Δ*sthABCDE*	This study
SPN201	IR715 Δ*stiABCH*	This study
SPN202	IR715 Δ*stjEDCBA*::KSAC	This study
SPN226	IR715 Δ*bcfABCDEFGH*::pSF1	This study
SPN227	IR715 Δ*fimAICDHF*::pSPN22	This study
SPN230	IR715 Δ*safABCD*	This study
SPN231	IR715 Δ*stbABCD*::pSF38	This study
SPN233	IR715 Δ*stdAB*::pSPN3	This study
SPN234	IR715 Δ*stfACDEFG*::pSF5	This study
SPN235	IR715 Δ*sthABCDE*::pSF25	This study
SPN236	IR715 Δ*stiABCH*::pSPN2	This study
SPN237	IR715 Δ*stjEDCBA*	This study
SPN251	IR715 Δ*safABCD*::pSPN13	This study
SPN252	IR715 Δ*stjEDCBA*::pSPN14	This study
SPN334	IR715 Δ*pefACD-orf5-orf6*::KSAC	This study
SPN335	IR715 Δ*pefACD-orf5-orf6*	This study
SPN336	IR715 Δ*pefACD-orf5-orf6*::pSPN16	This study
SPN337	IR715 Δ*stcABCD*::KSAC	This study
SPN338	IR715 Δ*stcABCD*	This study
SPN339	IR715 Δ*stcABCD*::pSPN15	This study
SPN365	SR11 Δ*fimAICDHF*	This study
SPN366	SR11 Δ*fimAICDHF* Δ*stbABCD*	This study
SPN367	SR11 Δ*fimAICDHF* Δ*stbABCD* Δ*sthABCDE*	This study
SPN368	SR11 Δ*fimAICDHF* Δ*stbABCD* Δ*sthABCDE* Δ*stfACDEFG*	This study
SPN369	SR11 Δ*fimAICDHF* Δ*stbABCD* Δ*sthABCDE* Δ*stfACDEFG* Δ*stiABCH*	This study
SPN370	SR11 Δ*fimAICDHF* Δ*stbABCD* Δ*sthABCDE* Δ*stfACDEFG* Δ*stiABCH* Δ*bcfABCDEFGH*	This study
SPN371	SR11 Δ*fimAICDHF* Δ*stbABCD* Δ*sthABCDE* Δ*stfACDEFG* Δ*stiABCH* Δ*bcfABCDEFGH* Δ*safABCD*	This study
SPN372	SR11 Δ*fimAICDHF* Δ*stbABCD* Δ*sthABCDE* Δ*stfACDEFG* Δ*stiABCH* Δ*bcfABCDEFGH* Δ*safABCD* Δ*pefACD-orf5-orf6*	This study
SPN373	SR11 Δ*fimAICDHF* Δ*stbABCD* Δ*sthABCDE* Δ*stfACDEFG* Δ*stiABCH* Δ*bcfABCDEFGH* Δ*safABCD* Δ*pefACD-orf5-orf6* Δ*stcABCD*	This study
SPN374	SR11 Δ*fimAICDHF* Δ*stbABCD* Δ*sthABCDE* Δ*stfACDEFG* Δ*stiABCH* Δ*bcfABCDEFGH* Δ*safABCD* Δ*pefACD-orf5-orf6* Δ*stcABCD* Δ*stjEDCBA*	This study
SPN375	SR11 Δ*fimAICDHF* Δ*stbABCD* Δ*sthABCDE* Δ*stfACDEFG* Δ*stiABCH* Δ*bcfABCDEFGH* Δ*safABCD* Δ*pefACD-orf5-orf6* Δ*stcABCD* Δ*stjEDCBA* Δ*stdAB*	This study
SPN376 (=SR11 Δ12)	SR11 Δ*fimAICDHF* Δ*stbABCD* Δ*sthABCDE* Δ*stfACDEFG* Δ*stiABCH* Δ*bcfABCDEFGH* Δ*safABCD* Δ*pefACD-orf5-orf6* Δ*stcABCD* Δ*stjEDCBA* Δ*stdAB* Δ*lpfABCDE*::KSAC	This study
MvP493	Δ*SPI4*::*aph*	15
MvP681	Δ*sadA*::*aph*	67
MvP702	Δ*wzz*::*aph*	46
MvP703	Δ*fepE*::*aph*	46
MvP813	Δ*invC*::*aph*	68
MvP886	Δ*rfaL*::*aph*	69

(Continued on next page)

TABLE 1 (Continued)

Strain	Relevant characteristics	Reference or source
MvP1208	Δ*sopB*::*aph*	70
MvP1209	Δ*cheY*::*aph*	71
MvP1210	Δ*fliI*::*aph*	71
MvP1412	Δ*sopE2*::*aph*	18
MvP1472	Δ*sopA*::*aph*	This study, construction intermediate
MvP1527	Δ*cheZ*::*aph*	71
MvP1611	Δ*bapABCD*::*aph*	This study, construction intermediate
MvP1663	Δ*sadA*::*aph*	This study, construction intermediate
MvP1754	Δ*fliC*::*aph*	72
MvP1755	Δ*fljB*::*aph*	72
MvP1760	Δ*fliC* Δ*fljB*::*aph*	72
MvP1825	Δ*shdA*::*aph*	This study
MvP1827	Δ*misL*::*aph*	This study
MvP1842	P_{tetA}::*shdA*	This study, construction intermediate
MvP1884	Δ*sipA*::*aph*	18
MvP1885	Δ*sopD*::aph	This study, construction intermediate
MvP2050	Δ*motAB*::*aph*	73
MvP2447	Δ12 Δ*misL*	This study
MvP2448	Δ12 Δ*misL* Δ*shdA*::*aph*	This study, construction intermediate
MvP2449	Δ12 Δ*misL* Δ*shdA*	This study, construction intermediate
MvP2456	Δ12 Δ*misL* Δ*shdA* ΔSPI4::*aph*	This study, construction intermediate
MvP2457	Δ12 Δ*misL* Δ*shdA* ΔSPI4	This study, construction intermediate
MvP2458	Δ12 Δ*misL* Δ*shdA* Δ*SPI4* Δ*bapABCD*::*aph*	This study, construction intermediate
MvP2486	Δ12 Δ*misL* Δ*shdA* ΔSPI4 Δ*bapABCD*	This study, construction intermediate
MvP2487	Δ12 Δ*misL* Δ*shdA* ΔSPI4 Δ*bapABCD* Δ*sadA*::*aph*	This study, construction intermediate
MvP2488	Δ12 Δ*misL* Δ*shdA* ΔSPI4 Δ*bapABCD* Δ*sadA*	This study, construction intermediate
MvP2506	Δ12 *rck*::*aph*-I-SceI	This study
MvP2507	Δ12 *pagN*::*aph*-I-SceI	This study
MvP2508	Δ*rck*::*aph*-I-SceI	This study
MvP2509	Δ*pagN*::*aph*-I-SceI	This study
MvP2518	Δ12 Δ*misL* Δ*shdA* Δ*SPI4* Δ*bapABCD* Δ*sadA* Δ*rck*::*aph*-I-SceI	This study, construction intermediate
MvP2535	Δ12 Δ*misL* Δ*shdA* ΔSPI4 Δ*bapABCD* Δ*sadA* Δ*rck*	This study, construction intermediate
MvP2533	Δ12 Δ*misL* Δ*shdA* ΔSPI4 Δ*bapABCD* Δ*sadA* Δ*rck* Δ*pagN*::*aph*-I-SceI	This study, construction intermediate
MvP2537	Δ12 Δ*misL* Δ*shdA* ΔSPI4 Δ*bapABCD* Δ*sadA* Δ*rck* Δ*pagN*	This study
MvP2622	Δ12 *shdA*::*aph*	This study
MvP2623	Δ12 *sadA*::*aph*	This study
MvP2624	Δ12 SPI4::*aph*	This study
MvP2625	Δ12 *bapABCD*::*aph*	This study
MvP2702	Δ*csgBAC-DEFG*::*aph*	This study, construction intermediate
MvP2703	Δ12 *csgBAC-DEFG*::*aph*	This study
MvP2706	Δ12 Δ*misL* Δ*sadA* Δ*shdA* ΔSPI4 Δ*bapABCD* Δ*rck* Δ*pagN* Δ*csgBAC-DEFG*::*aph*	This study, construction intermediate
MvP2707 (=SR11 Δ20)	Δ12 Δ*misL* Δ*sadA* Δ*shdA* ΔSPI4 Δ*bapABCD* Δ*rck* Δ*pagN* Δ*csgBAC-DEFG*	This study
MvP2710	Δ12 Δ*misL* Δ*sadA* Δ*shdA* ΔSPI4 Δ*bapABCD* Δ*rck* Δ*pagN* Δ*csgBAC-DEFG* Δ*fliI*::*aph*	This study
MvP2711	Δ12 Δ*misL* Δ*sadA* Δ*shdA* ΔSPI4 Δ*bapABCD* Δ*rck* Δ*pagN* Δ*csgBAC-DEFG* Δ*motAB*::*aph*	This study
MvP2718	Δ12 Δ*invC*::*aph*	This study
MvP2788	Δ12 Δ*fepE*::*aph*	This study, construction intermediate
MvP2789	Δ12 Δ*wzz*::*aph*	This study, construction intermediate
MvP2790	Δ12 Δ*rfaL*::*aph*	This study, construction intermediate
MvP2798	Δ12 Δ*fepE*	This study
MvP2799	Δ12 Δ*wzz*	This study
MvP2800	Δ12 Δ*rfaL*	This study
MvP2812	Δ12 Δ*fepE* Δ*wzz*::*aph*	This study
MvP2819	Δ12 Δ*sopB*::*aph*	This study, construction intermediate
MvP2828	Δ12 Δ*sopB*	This study, construction intermediate
MvP2829	Δ12 Δ*sopB* Δ*sopA*::*aph*	This study, construction intermediate
MvP2831	Δ12 Δ*sopB* Δ*sopA*	This study, construction intermediate
MvP2832	Δ12 Δ*sopB* Δ*sopA* Δ*sopE2*::*aph*	This study, construction intermediate
MvP2835	Δ12 Δ*sopB* Δ*sopA* Δ*sopE2*	This study, construction intermediate
MvP2841	Δ12 Δ*sopB* Δ*sopA* Δ*sopE2* Δ*sopD*::*aph*	This study, construction intermediate
MvP2843	Δ12 Δ*sopB* Δ*sopA* Δ*sopE2* Δ*sopD*	This study, construction intermediate
MvP2844 (=SR11 Δeffector proteins)	Δ12 Δ*sopB* Δ*sopA* Δ*sopE2* Δ*sopD* Δ*sipA*::*aph*	This study
MvP2864	Δ12 Δ*misL*::*aph*	This study

TABLE 2 Plasmids used in this study

Plasmid	Relevant genotype	Reference or source
pE-FLP	FLP recombinase expression	74
pKD4	*aph* resistance cassette flanked by FRT sites; Km^r $Carb^r$	58
pKD13	*aph* resistance cassette flanked by FRT sites, temp-sensitive replication (30°C); Km^r $Carb^r$	58
pWRG730	Red recombinase expression	59
p3313	pWSK29 *rfaDFCL*	69
p3773	*tetR* P_{tetA}	31
p4253	*tetR* P_{tetA}::*bapABCD* in pWSK29	31
p4318	*tetR* P_{tetA}::*bapA*[ΔBlg1]*BCD* in pWSK29	This study
p4321	*tetR* P_{tetA}::*bapA*[ΔBlg28]*BCD* in pWSK29	This study
p4320	*tetR* P_{tetA}::*bapA*[ΔBlg15-24]*BCD* in pWSK29	This study
p4331	*tetR* P_{tetA}::*bapA*[ΔBlg1-28]*BCD* in pWSK29	This study
p4380	*tetR* P_{tetA}::*csgBACEFG* in pWSK29	31
p4389	*tetR* P_{tetA}::*stiABCD* in pWSK29	31
p4390	*tetR* P_{tetA}::*stfABCDEFG* in pWSK29	31
p4391	*tetR* P_{tetA}::*stbABCDEFG* in pWSK29	31
p4392	*tetR* P_{tetA}::*fimAICDHF* in pWSK29	31
p4393	*tetR* P_{tetA}::*safABCD* in pWSK29	31
p4394	*tetR* P_{tetA}::*stdABCD* in pWSK29	31
p4395	*tetR* P_{tetA}::*stjABCDE* in pWSK29	31
p4396	*tetR* P_{tetA}::*pefACDEF* in pWSK29	31
p4397	*tetR* P_{tetA}::*bcfABCDEFG* in pWSK29	31
p4399	*tetR* P_{tetA}::*stcABC* in pWSK29	31
p4400	*tetR* P_{tetA}::*sthABCDE* in pWSK29	31
p4401	*tetR* P_{tetA}::*pagN* in pWSK29	31
p4402	*tetR* P_{tetA}::*rck* in pWSK29	31
p4403	*tetR* P_{tetA}::*misL* in pWSK29	31
p4519	*tetR* P_{tetA}::*lpfABCDE* in pWSK29	31
p4520	*tetR* P_{tetA}::*shdA* in pWSK29	31
p4904	*tetR* P_{tetA}::*hilD* in pWSK29	This study
p5035	*tetR* P_{tetA}::*sadBA* in pWSK29	This study
pBluescriptII KS+	Cloning vector; $Carb^r$	75
pBS34	pBluescriptII KS+ [XbaI][PstI]KSAC[PstI][XbaI]); $Carb^r$ Km^r	76
pCR2.1	TOPO TA cloning vector; $Carb^r$ Km^r	Invitrogen
pEW5	pRDH10 Δ*stdAB* (−60 to +3219)::KSAC; Cm^r Tet^r Km^r	12
pEW13	pRDH10 Δ*stiABCH* (+40 to +4992)::KSAC); Cm^r Km^r	12
pRDH10	$oriV_{R6K}$ *sacRB* mob_{RP4}; Cm^r Tet^r	77
pSF1	pRDH10 Δ*bcfABCDEFGH* (+47 to +6830); Cm^r Tet^r	12
pSF2	pRDH10 Δ*fimAICDHF* (+40 to +5970); Cm^r Tet^r	66
pSF5	pRDH10 Δ*stfACDEFG* (−122 to +5493); Cm^r Tet^r	12
pSF25	pRDH10 Δ*sthABCDE* (−6 to +5420); Cm^r Tet^r	12
pSF38	pRDH10 Δ*stbABCD* (−59 to +5183); Cm^r	12
pSPN2	pEW13 Δ*stiABCH* (+40 to +4992); Cm^r	This study
pSPN3	pEW5 Δ*stdAB* (−60 to +3219); Cm^r Tet^r	This study
pSPN5	pCR2.1 (LPF-FR1); $Carb^r$ Km^r	This study
pSPN6	pCR2.1 Δ*safABCD* (−45 to +4364); $Carb^r$ Km^r	This study
pSPN7	pCR2.1 Δ*stjEDCBA* (−49 to +5185); $Carb^r$ Km^r	This study
pSPN8	pCR2.1 Δ*stcABCD* (−65 to +4827); $Carb^r$ Km^r	This study
pSPN9	pCR2.1 Δ*pefACD-orf5-orf6* (−110 to +5610); $Carb^r$ Km^r	This study
pSPN12	pCR2.1 (LPF-FR2); $Carb^r$ Km^r	This study
pSPN13	pRDH10 Δ*safABCD* (−45 to +4364); Cm^r	This study
pSPN14	pRDH10 Δ*stjEDCBA* (−49 to +5185); Cm^r	This study
pSPN15	pRDH10 Δ*stcABCD* (−65 to +4827); Cm^r	This study
pSPN16	pRDH10 Δ*pefACD-orf5-orf6* (−110 to +5610); Cm^r	This study
pSPN17	pBluescriptII KS+ ([BamHI]LPF-FR1[PstI]); $Carb^r$	This study
pSPN18	pSPN13 Δ*safABCD* (−45 to +4364)::KSAC); Cm^r Km^r	This study
pSPN19	pSPN14 Δ*stjEDCBA* (−49 to +5185)::KSAC); Cm^r Km^r	This study
pSPN20	pSPN15 Δ*stcABCD* (−65 to +4827)::KSAC); Cm^r Km^r	This study
pSPN21	pSPN16 Δ*pefACD-orf5-orf6* (−110 to +5610)::KSAC); Cm^r Km^r	This study
pSPN22	pRDH10 Δ*fimAICDHF* (+40 to +5970); Cm^r	This study
pSPN26	pSPN17 ([BamHI]LPF-FR1[PstI]LPF-FR2[Acc65I]); $Carb^r$	This study
pSPN27	pRDH10 Δ*lpfABCDE* (−60 to +5325); Cm^r	This study
pSPN37	pSPN27 Δ*lpfABCDE* (−60 to +5325)::KSAC); Cm^r Km^r	This study

TABLE 3 Oligonucleotides used in this study

Oligonucleotide	Sequence (5′–3′)	Purpose and/or target
Gibson assembly		
1r-ST-Ptet-sadA-pWSK29	CCGGGCTGCAGGAATTCATGGCATTATGCCATTGC	*sadBA*
1f-ST_Ptet-fim-pWSK29	TCGACGGTATCGATAAGCTTAGGGAAAAAGGTTATGCTGCT	*sadBA*
Vf-pWSK29	GAATTCCTGCAGCCCGGGG	Vector p4392
Vr-pWSK29-Ptet-rev	TTCACTTTTCTCTATCACTGATAGGGAGTGGTAAAATAACTCT	Vector p4392
1f-PtetA-hilD	CCCTATCAGTGATAGAGAAAAGTGAAAACATCAACAAAGGGATAATATG	*hilD*
1r-hilD-vec	CCCGGGCTGCAGGAATTCTGCCTGGCAGAAAGCTA	*hilD*
Vr-PtetA	TTCACTTTTCTCTATCACTGATAGGGAGTGGTA	Vector p4252
hVPS26B-Rev-EcoRI	TCAGAATTCTCTGCCTGCAGTTGTTGTCAGACAGC	Vector pWSK29
Vr-pWSK29	AAGCTTATCGATACCGTCGACCTC	Vector pWSK29
1f-FRT	CGACGGTATCGATAAGCTTGAAAGTTCCTATACTTTCTAGAGAATA	P_{tetA}-*misL*
1r-misL	CCCGGGCTGCAGGAATTCCATGAAACCTATCAGCCAAA	P_{tetA}-*misL*
Site-directed mutagenesis		
ST-delbapA-Big1-Q5-fw	CCTCTCCCCGATACACCG	SDM p4253
ST-delbapA-Big1-Q5-rv	AGTATCTACAGGATTACTGCTACC	SDM p4253
ST-delbapA-Big28-Q5-fw	ATAACCAGTCTTGATCTGAC	SDM p4253
ST-delbapA-Big28-Q5-rv	CGTATCGACAATCACCGTC	SDM p4253
ST-delbapA-Big15-Q5-rv	GGTGTCGACGGTGAAGGTAAAGCTG	SDM p4253
ST-delbapA-Big24-Q5-fw	CTTGCGCCAACGGTTCCG	SDM p4253
Check of P22 transductions and *aph* cassette removal		
K1-Red-Del	CAGTCATAGCCGAATAGCCT	*aph*
K2-Red-Del	CGGTGCCCTGAATGAACTGC	*aph*
CsgC-Check-rev	TGTTGCCCTACCGCAGAATG	*csgBAC*
CsgG-Del-Check-for	AGTGGGCTATGGCTGGCATC	*csgBAC-DEFG*
SPI4-Ctrl-For	CGGTAGAGAATGGTCGGTAT	SPI4
SPI4-Ctrl-Rev	GTGCTGACCTGATACGCTAT	SPI4
InvC-DelCheck-For	TGTATCAGCGTCAAGGACGA	*invC*
InvC-DelCheck-Rev	CGGCGAACAATAGACTGCTT	*invC*
SopB-DelCheck-Rev	CAATGGCATAAAGGGACAGC	*sopB*
SopB-DelCheck-For	TACGTATGGACGTCAGGATG	*sopB*
FLiI-DelCheck-For	CGATCCAACGTTGCATCACG	*fliI*
FliI-DelCheck-Rev	ACGCATTTCGCCCAGTAAAC	*fliI*
sopE2-check-rev4	GCGTCGCCATAAAAACGAATA	*sopE2*
SopE2-Red-Check-For	TGTGACGCAGTAGTTGAATTGAAG	*sopE2*
sopA-DelCheck-Rev	TTCGTACATGCGATGGTGAG	*sopA*
SopA-Check-For	CCTGCCAGATAACATGGTGAATT	*sopA*
BapA-Check-For	GTCAGGCACAAAAAACAAAGGGT	*bapABCD*
bapD-Check-Rev	CCGAAATTCCTACATCCTCGG	*bapABCD*
STM3690-sadA-For	GAGCATGGACAAACGTCACGC	*sadA*
SadA-end-Rev	GGCATTATGCCATTGCCTTTG	*sadA*
ShdA-DelCheck-For	GCCACAGCAAAGTTAAAGCG	*shdA*
ShdA-DelCheck-Rev	TGAAGTCAAATCCGTCACGC	*shdA*
MisL-DelCheck-For	TTTATGTGCATAAGCTGCGG	*misL*
MisL-DelCheck-Rev	CAGGGCCATCGTGGCTTTAT	*misL*
SipA-Red-Check-For	CACATTACAGACGCTGACGC	*sipA*
sopD-DelCheck-For	ACCACAAAGGATTACCAACC	*sopD*
sopD-DelCheck-For	GGCTGCATGAAGGGTAATTG	*sopD*
MotB-Check-Rev	CCTGCAGAATAGTGAAGCCG	*motAB*
MotA-Check-For	ATGAACAGATCGAACAGG	*motAB*
pagN-check-for	CGTAGAAGTGAAACCGTACG	*pagN*
pagN-check-rev	CAGCTATTTTACCGATAGTG	*pagN*
rck-check-for	GAGGATGAAGCGGCGTTACG	*Rck*
rck-check-rev	GTACCACACCACAAACCAGC	*Rck*
FliC-For-XhoI	GCGCTCGAGGCAAACAGTAGTTAAGCGCG	*fliC*
FliC-Rev-EcoRI	AGCGAATTCAGCTTTCGCTGCCTTGATTG	*fliC*
FljB-For-XhoI	AGTCTCGAGCAATTTGCACTAGTAAGCGC	*fljB*
FljB-Rev	GCAAGCATAGAATAATCCCG	*fljB*
CheZ-Check-For	AAAACCATTCGCGCCGATAG	*cheZ*
CheZ-Check-Rev	GGTAAAAAAGGCGGGGTTTAT	*cheZ*
CheY-DelCheck-Rev	TACCGATGCGCGCAATGATG	*cheY*
CheY-DelCheck-For	ACGAAGCAAGTTGTGTGGTG	*cheY*
Wzz-FepE-DelCheck-For	AAACTATCGGGCCCATCATC	*fepE*

(Continued on next page)

TABLE 3 (Continued)

Oligonucleotide	Sequence (5′–3′)	Purpose and/or target
Wzz-FepE-DelCheck-Rev	TGTTAAGCGATCTCAACCGC	*fepE*
WzzB-DelCheck-For	AAAAGTGTATACCCGCGATC	*wzz*
WzzB-DelCheck-Rev	AGTGATGTAGTGGCATTGAG	*wzz*
RfaL-DelCheck-For	GCTGGCTGGCGCAAAATTTG	*rfaL*
RfaL-DelCheck-Rev	TATTGTGCCATCTCAGGTTG	*rfaL*
Red deletion		
CsgC-Red-del-rev	CCGCCACCATCAAAAACTACTGTGCAGAAGGCGGCCATTGTGTAGGCTGGAGCTGCTTCG	*csgBAC*
CsgG-Red-Del-for	CACGCTTTGTCGTATTCATCAGGATTCTGGCGGTACTGACATTCCGGGGATCCGTCGACC	*csgBAC-DEFG*
misL-Del13-For	AGACGCTTTACGCCATAATGCAGGAGGCAGAATGCCAACTATTCCGGGGATCCGTCGACC	*misL*
misL-Del13-Rev	ATCAGCGGCTCTGTTGTTACCTGAATCAGAAACTGTATTTTGTAGGCTGGAGCTGCTTCG	*misL*
ShdA-Del13-For	AATAAAAGCAACGCGCGCGGCGCTGGCTTGCGCCGTGGCTATTCCGGGGATCCGTCGACC	*shdA*
ShdA-Del13-Rev	GGCAGGGAACACCCGCCCGGTTTTGTCTAACTTACCAGTTTGTAGGCTGGAGCTGCTTCG	*shdA*
pagN-del-red-for	GAAACTTGTCTTTTAGCCCAATATTAAGGCAGGTTCTGAAAGGGTTTTCCCAGTCACGAC	*pagN*
pagN-del-red-rev	CATGAAGTCATTGGAGGCAGCCTTTGTGTCTGCATCATAATGCTTCCGGCTCGTATGTTG	*pagN*
rck-del-red-for	CATAACACAATGAACTTAACTGTGTTCAGGGAGTTTTATCAGGGTTTTCCCAGTCACGAC	*rck*
rck-del-red-rev	CGGAAGCCTGCGGCTCCGCTCCCTTTCCTGCTCTCCGTTATGCTTCCGGCTCGTATGTTG	*rck*
misL-Red-Ptet-For	TTTTATAGATCCGTTTCCATTTTTATTATTTCCATATTATTGTAGGCTGGAGCTGCTTCG	*tetR* P_{tetA}
misL-Red-Ptet-Rev	ATGAGTAATTTTGGGGAGTTGGCATTCTGCCTCCTGCATTTTCACTTTTCTCTATCACTG	*tetR* P_{tetA}
BapB-Del-Red-For	GTTCGGGGCAACAAGCGGTGATATTTAAAAGGGATAAACTGTGTAGGCTGGAGCTGCTTC	*bapABCD*
BapD-Del-Red-Rev	CACGCGTGACCAGCCCCCGTATCTTCTTATCTTCAACGATCATATGAATATCCTCCTTAG	*bapABCD*
SopA-Red-DEl13-For	CCAGACCGTTTTTCCATAATGATGTTGATAAGGAATTCTAATTCCGGGGATCCGTCGAC	*sopA*
SopA-Red-Del13-Rev	CAACGCTGTGTCCCTTAATTCCATGCGGGTTGAGGCTGGAGTAGGCTGGAGCTGCTTCG	*sopA*
sopD-Del13-For	GATATTGAATAATATAAATTTGAAGGAAAATATTATGCCAATTCCGGGGATCCGTCGACC	*sopD*
sopD-Del13-rev	CAGCCGGATTTTAAATTGGTTATATTACTGACTATCTTTATGTTGTAGGCTGGAGCTGCT	*sopD*
Δ12 construction: PCR primers for cloning flanking regions		
100-LPF6-Bam	TATCGGGGATCCGGGTTGAGTCGTATGACC	*lpf* flanking region 1
63-LPF5-Pst	TATGCGCTGCAGGTGTATAGAGGTGGGTATTGG	*lpf* flanking region 1
64-LPF3-Pst	TATCGCCTGCAGCATCTGGTGGGGAGCAACAATAC	*lpf* flanking region 2
101-LPF7-Bam	TATCGGGGATCCGCCAAACAGTGAAAGAAGACGAAG	*lpf* flanking region 2
66-SAF1-Bam	ATAGGCGGATCCCTGCACTGAAAAGCGATACC	*saf* flanking region 1
67-SAF2-Xba	ATAGGCTCTAGAACGCCATACCAAATCTTACC	*saf* flanking region 1
92-SAF5-Xba	TATCGCTCTAGACTGTTCCACTCATACTTCC	*saf* flanking region 2
69-SAF4-Bam	TATGCGGGATCCTGGTCACAAGAAAGAGATGC	*saf* flanking region 2
70-STJ1-Bam	TTACGCGGATCCCCTTTTTCGCCCATTACG	*stj* flanking region 1
71-STJ2-Xba	TATCGGTCTAGAGGTCGGGATTCTATGAAG	*stj* flanking region 1
72-STJ3-Xba	TATCGGTCTAGAGAAGTGCTGACGAAATAAACG	*stj* flanking region 2
73-STJ4-Bam	ATACGCGGATCCGGCATGTTAGGTTTCACC	*stj* flanking region 2
78-STC5-Bam	TTTGCGGGATCCAAGAGAATATGACATTCACTGC	*stc* flanking region 1
79-STC6-Xba	ATAGCCTCTAGACATAGACAGGAAGTTATCGC	*stc* flanking region 1
80-STC7-Xba	ATAGGCTCTAGACGATAGGTGAATGAACTTCC	*stc* flanking region 2
81-STC8-Sal	TATGCCGTCGACCAGCAGAAATGATACACACG	*stc* flanking region 2
88-PEF5-Bam	TTTGGCGGATCCTAATCTCACAGCCCGAAGC	*pef* flanking region 1
89-PEF6-Xba	ATTGCCTCTAGACAGCTATGACGTGACATCG	*pef* flanking region 1
90-PEF7-Xba	ATAGCGTCTAGAATGCGTGGTGTACTGAGG	*pef* flanking region 2
91-PEF8-Sal	TAAGGGGTCGACGGCAGAAATGGTTTTGACG	*pef* flanking region 2
Δ12 construction: PCR primers for confirmation of deletions		
34-KSAC-5out	GGCATAAATTCCGTCAGC	Amplify out KSAC 5′ end
35-KSAC-3out	TGATGACGAGCGTAATGG	Amplify out KSAC 3′ end
38-BCF-Up1	CATGATGACAAACGACTCC	*bcf* deletions
39-BCF-Down1	CGCCATTTGCAACATATCC	*bcf* deletions
40-FIM-Up1	CGTCTACGTCTTTATCTGG	*fim* deletions
41-FIM-Down1	GCACTTATCCTGTTGACC	*fim* deletions
42-LPF-Up1	GGGAGAATATCTGGAAAGC	*lpf* deletions
43-LPF-Down1	CAGCCACAATACAAAGTGC	*lpf* deletions
44-PEF-Up1	CGACAGGATATTTGCTCC	*pef* deletions
45-PEF-Down1	GTCAGTTTCCTTCATCACC	*pef* deletions
46-STB-Up1	ATATGTTCTCCCGAGTCG	*stb* deletions
47-STB-Down1	GTATGGCGGTATATTGTCG	*stb* deletions

(Continued on next page)

TABLE 3 (Continued)

Oligonucleotide	Sequence (5′–3′)	Purpose and/or target
48-STC-Up1	GGGGATATTCAGCTAACG	*stc* deletions
49-STC-Down1	GAGATCCAGGCAAAATCG	*stc* deletions
50-STD-Up1	TTCAGCAAACCCGTAAGG	*std* deletions
51-STD-Down1	GTGTAGCGATTCATCTGC	*std* deletions
52-STF-Up1	GCGTTTTACTGGTCTTTGC	*stf* deletions
53-STF-Down1	GTATCAACGGGAACTTTCG	*stf* deletions
54-STH-Up1	CCTTGTAGATGCCTATGC	*sth* deletions
55-STH-Down1	GGATTGGGACAACTTACC	*sth* deletions
56-STI-Up1	CAGAGACTGGTGACATCC	*sti* deletions
57-STI-Down1	AAGCTGAAATCGGAGACG	*sti* deletions
74-SAF-Up1	TATGATACCGAAGGAATACC	*saf* deletions
75-SAF-Down1	TCGACACGAAGCAAATCC	*saf* deletions
76-STJ-Up1	ACCCATGAACAGGTCTGC	*stj* deletions
77-STJ-Down1	ACTGAAGATGGCAACTCC	*stj* deletions
Δ12 construction: PCR primers to check for presence of predicted major subunit		
145-bcfA1	GATACTACAACCGTCACT	*bcfA* presence
146-bcfA2	CCAACAGACGAGAAAAAAATCCCG	*bcfA* presence
147-fimA1	GCTGATCCTACTCCGGTG	*fimA* presence
148-fimA2	AAAATGGAACGCTGACGGGAGC	*fimA* presence
149-stbA1	GTTTCTGATAACACCATC	*stbA* presence
150-stbA2	GCTACCCAAAATAGTAACGCTCGC	*stbA* presence
151-stfA1	GCGGGCAGTAATACTGGT	*stfA* presence
152-stfA3	AGCCAGAACAATACCCACCACG	*stfA* presence
153-sthA1	TCCACACCGGTATTTGC	*sthA* presence
154-sth-II	GGCATCAAGGCGAAAAAGAGG	*sthA* presence
155-stiA	CAACAGGCAACAAAGCAACCC	*stiA* presence
156-stiC	CCGCCAAAGACGGCACCG	*stiA* presence
157-safA1-Bam	TTAGCGGGATCCGGCTCATTTTTGCCGAACTC	*safA* presence
158-safA2-Sal	TTCACCGTCGACTTAAGGTTGATATCCCACTACG	*safA* presence
159-stjE1-Bam	TTAGCGGGATCCGTTGAATCCACTGCTGTATTAAAACTG	*stjE* presence
160-stjE2-Sal	TATGCCGTCGACCTGGTTGTAGCAAAGGAAGC	*stjE* presence
161-lpfA1	GCTGAATCTGGTGACGGC	*lpfA* presence
162-lpfA2	GATTCTCTTCCTGAGCCTCCG	*lpfA* presence
163-pefA1	GCCAATGAAGTAACTTTCCTGG	*pefA* presence
164-pefA2	GTTCTGCTTACGGGGGATTATTTG	*pefA* presence
165-stcA1	GTTGATGAGTATGATTCAGGC	*stcA* presence
166-stcA2	AACGACTTCTTTCTTCTCTGCCG	*stcA* presence
167-stdAF	GCCGATACTACACCCACAGC	*stdA* presence
168-stdA2	CGACTTCAGGACGGAAAATGTC	*stdA* presence

integrated into the genome were selected for on LB-Cm-Nal agar, and colonies were then transferred to 5% sucrose agar (56) and incubated at 30°C. Sucrose-resistant (Suc^r) colonies lacking the pRDH10(Δ) vector and the Δ::KSAC locus were identified by screening for a Km^s Cm^s phenotype, and the presence of the unmarked deletion was then validated by obtaining the expected PCR product size when amplifying over the deleted region. To enable transduction of the unmarked deletions (57), we next generated IR715 Δ::pRDH10::Δ strains (e.g., SPN251 = IR715 Δ*saf*::pSPN13), thus reversibly marking the unmarked deletion with the Cm-selectable, sucrose-counterselectable pRDH10 suicide vector. The respective pRDH10(Δ) construct was thus conjugated back into the relevant IR715 unmarked deletion strain, transconjugants with the plasmid integrated into the genome were selected for on LB-Cm-Nal agar, and plasmid integration was further inferred by the inability to PCR amplify across the respective unmarked deletion region due to the size increase.

The *S.* Typhimurium SR11 strain with a deletion of all 12 chaperone-usher fimbrial gene clusters (Δ12; SPN376) was then generated, with a focus on minimizing the number of passages necessary for introducing each deletion. To begin, Δ*fim*::pSPN22 of SPN227 was transduced via phage P22 HT105/1 *int*-201 into wild-type SR11, and transductants were selected for on LB-Cm agar. As SR11 accepts DNA from P22 but is resistant to lysis by the phage, phage cleanup was unnecessary. Transductants were thus struck immediately to 5% sucrose agar and incubated at 30°C. Suc^r colonies were then screened for Cm^s by streaking for single-colony isolation on both LB agar and LB-Cm agar. Colony PCR was performed to confirm Δ*fim* status (positive for amplification across the unmarked deletion and negative for *fimA* amplification) of Suc^r Cm^s colonies. A validated colony was then grown in LB medium, an aliquot of which was used for creating a freezer stock (SPN365 = SR11 Δ*fim*) and another aliquot of which was used in the next round of transduction. This process was then repeated for the remaining deletions. The unmarked deletions were transduced first, generating strains SPN366 to SPN375. For the final deletion,

Δ*lpf*::KSAC of SPN193 was transduced, yielding the Δ12 strain (SPN376). With each successive deletion, every deletion thus far introduced into the strain was reconfirmed by PCR, as was the expected presence/absence of every major fimbrial subunit gene.

Construction of strains and plasmids. For introduction of the genes *sadBA* under the Tet-on system, template vector p4392 harboring *tetR* P_{tetA}::*fimAICDHF* was used. Amplification of *sadBA* from the genome of *S.* Typhimurium NCTC 12023 and the vector including the Tet-on system *aph tetR* P_{tetA} present on p4392 was done using oligonucleotides as listed in Table 3, and the PCR products were purified by PCR purification (NEB; Monarch). The PCR product containing *sadBA* and the PCR product from vector p4392 were assembled by Gibson assembly according to the manufacturer's protocol (NEB; Monarch). For overexpression of the *sii* operon, a plasmid was generated for Tet-on expression of transcriptional regulator *hilD*. Using primers listed in Table 3, *hilD* was amplified from *S.* Typhimurium NCTC 12023 genomic DNA, and the vector including *aph tetR* P_{tetA} present on p4392 was amplified as described before.

Strains with deletion of *csgBAC-DEFG*, *rck*, and *pagN* were created using λ Red recombination in *S.* Typhimurium 12023 harboring pWRG730. One-step gene inactivation was performed as described previously (58) using oligonucleotides as listed in Table 3. Deletion was checked by colony PCR using oligonucleotides as listed in Table 3. Further deletion of *aph* was performed using pE-FLP encoding FLP recombinase as described (58). For strains lacking *rck* and *pagN*, further deletion of *aph* was performed using I-SceI counterselection as described previously (59). Generation of strains lacking all fimbrial operons (SR11 Δ12) and one further adhesive structure were created by transferring the deletion by P22 phage transduction. The several deletions were always checked by colony PCR using oligonucleotides as listed in Table 3.

Cultivation of sterile grown corn salad. Corn salad seeds (*Valerianella locusta* Verte à cour plein 2, N.L. Chrestensen Erfurter Samen- und Pflanzenzucht) were kindly provided by Adam Schikora and Sven Jechalke (Justus Liebig University Giessen). Seeds were sterilized with 70% ethanol (EtOH) for 1 min followed by 3% NaClO for 2 min. Seeds were washed thrice with sterile ultrapure water (MilliQ) and allowed to dry for 30 min. Seeds were planted on Murashige-Skoog (MS) agar (per liter: 2.2 g of Murashige-Skoog medium including vitamins [Duchefa Biochemie; number M0222], 10 g of agar, and 0.5 g of morpholineethanesulfonic acid [MES; pH 5.4]) in sterile plastic containers with air filters (round model, 140 mm [Duchefa Biochemie; number E1674]) at 20°C with a 12-h/12-h day/night cycle for 8 weeks.

Adhesion to corn salad. For infection of corn salad by *Salmonella*, leaf discs (8 mm average) of 8-week-old plants were punched out by biopsy punches immediately before infection process. Forty-eight-well plates were used with one leaf disc per well mechanically fixed by sterile stainless steel inlays. For each condition, three leaf discs were infected. For infection, overnight cultures of *Salmonella* strains were diluted 1:31 in LB (containing antibiotics if required) and grown for 3.5 h in test tubes with aeration in a roller drum. The cultures were diluted in phosphate-buffered saline (PBS) to obtain approximately 5.6×10^7 bacteria/ml, and 50 μl of this inoculum was spotted onto one leaf disc. The infection process was carried out either for 1 h at room temperature (RT) under static conditions or for 55 min at RT after a centrifugation step at $500 \times g$ for 5 min. After infection, leaf discs were washed once with PBS to remove nonbound bacteria. Three leaf discs were transferred to tubes and washed two further times with PBS by short mixing on a Vortex mixer. Plant tissue was homogenized with a pellet pestle motor in 600 μl of 1% sodium deoxycholate in PBS, and CFU were determined by plating serial dilutions of the lysates on MH agar plates (Mueller-Hinton agar plates) incubated overnight at 37°C. A noninfected sample was used in every assay to ensure the sterility of the corn salad.

Flow cytometry. For analysis of surface expression of SadA and BapA by flow cytometry, 6×10^8 bacteria were washed in PBS and then fixed with 3% paraformaldehyde–PBS for 20 min. Bacteria were blocked with 2% goat serum in PBS for 30 min and afterwards stained with the specific antiserum goat anti-SadA or goat anti-BapA diluted 1:250 and 1:1,000 in 2% goat serum-PBS for 2 h and goat anti-rabbit IgG antibody coupled to Alexa-Fluor 488 diluted 1:2,000 in 2% goat serum-PBS for 1 h. For analysis of surface expression of SiiE by flow cytometry, ca. 3×10^8 bacteria were fixed in 3% paraformaldehyde in PBS for 20 min. Bacteria were blocked with blocking solution (2% goat serum and 2% bovine serum albumin in PBS) for 30 min and afterwards stained with the specific antiserum anti-SiiE C-terminally coupled to Alexa-Fluor 488 (1:100) for 1 h. Bacteria were measured with an Attune NxT flow cytometer (Thermo Fisher) and analyzed using Attune NxT software version 2.7. A mutant strain lacking the respective adhesive structure was used as a negative control for gating.

SUPPLEMENTAL MATERIAL

Supplemental material is available online only.

SUPPLEMENTAL FILE 1, PDF file, 0.5 MB.

ACKNOWLEDGMENTS

This work was supported by the Bundesanstalt für Landwirtschaft und Ernährung (BLE) by project Plantinfect (grant 2813HS027). Further support by the DFG through grant SFB 944, project Z, is gratefully acknowledged.

We thank the members of the Plantinfect consortium for fruitful discussion and exchange of reagents. We thank Inigo Lasa and Dirk Linke for sharing antisera against BapA and SadA, respectively.

REFERENCES

1. Andino A, Hanning I. 2015. *Salmonella enterica*: survival, colonization, and virulence differences among serovars. ScientificWorldJournal 2015: 520179. https://doi.org/10.1155/2015/520179.
2. Hernandez-Reyes C, Schikora A. 2013. *Salmonella*, a cross-kingdom pathogen infecting humans and plants. FEMS Microbiol Lett 343:1–7. https://doi.org/10.1111/1574-6968.12127.
3. Brandl MT, Cox CE, Teplitski M. 2013. *Salmonella* interactions with plants and their associated microbiota. Phytopathology 103:316–325. https://doi.org/10.1094/PHYTO-11-12-0295-RVW.
4. Holden N, Pritchard L, Toth I. 2009. Colonization outwith the colon: plants as an alternative environmental reservoir for human pathogenic enterobacteria. FEMS Microbiol Rev 33:689–703. https://doi.org/10.1111/j.1574-6976.2008.00153.x.
5. EFSA Panel on Biological Hazards (BIOHAZ). 2014. Scientific Opinion on the risk posed by pathogens in food of non-animal origin. Part 2 (Salmonella and Norovirus in leafy greens eaten raw as salads). EFSA J 12:118.
6. Hanning IB, Nutt JD, Ricke SC. 2009. Salmonellosis outbreaks in the United States due to fresh produce: sources and potential intervention measures. Foodborne Pathog Dis 6:635–648. https://doi.org/10.1089/fpd.2008.0232.
7. Schikora A, Garcia AV, Hirt H. 2012. Plants as alternative hosts for Salmonella. Trends Plant Sci 17:245–249. https://doi.org/10.1016/j.tplants.2012.03.007.
8. Schikora A, Carreri A, Charpentier E, Hirt H. 2008. The dark side of the salad: *Salmonella typhimurium* overcomes the innate immune response of *Arabidopsis thaliana* and shows an endopathogenic lifestyle. PLoS One 3:e2279. https://doi.org/10.1371/journal.pone.0002279.
9. Jechalke S, Schierstaedt J, Becker M, Flemer B, Grosch R, Smalla K, Schikora A. 2019. Salmonella establishment in agricultural soil and colonization of crop plants depend on soil type and plant species. Front Microbiol 10:967. https://doi.org/10.3389/fmicb.2019.00967.
10. Jablasone J, Warriner K, Griffiths M. 2005. Interactions of *Escherichia coli* O157:H7, *Salmonella typhimurium* and *Listeria monocytogenes* plants cultivated in a gnotobiotic system. Int J Food Microbiol 99:7–18. https://doi.org/10.1016/j.ijfoodmicro.2004.06.011.
11. Wagner C, Hensel M. 2011. Adhesive mechanisms of *Salmonella enterica*. Adv Exp Med Biol 715:17–34. https://doi.org/10.1007/978-94-007-0940-9_2.
12. Humphries AD, Raffatellu M, Winter S, Weening EH, Kingsley RA, Droleskey R, Zhang S, Figueiredo J, Khare S, Nunes J, Adams LG, Tsolis RM, Bäumler AJ. 2003. The use of flow cytometry to detect expression of subunits encoded by 11 Salmonella enterica serotype Typhimurium fimbrial operons. Mol Microbiol 48:1357–1376. https://doi.org/10.1046/j.1365-2958.2003.03507.x.
13. Thanassi DG, Saulino ET, Hultgren SJ. 1998. The chaperone/usher pathway: a major terminal branch of the general secretory pathway. Curr Opin Microbiol 1:223–231. https://doi.org/10.1016/S1369-5274(98)80015-5.
14. Grund S, Weber A. 1988. A new type of fimbriae on *Salmonella typhimurium*. Zentralbl Veterinarmed B 35:779–782. https://doi.org/10.1111/j.1439-0450.1988.tb00560.x.
15. Gerlach RG, Jackel D, Stecher B, Wagner C, Lupas A, Hardt WD, Hensel M. 2007. Salmonella pathogenicity island 4 encodes a giant non-fimbrial adhesin and the cognate type 1 secretion system. Cell Microbiol 9:1834–1850. https://doi.org/10.1111/j.1462-5822.2007.00919.x.
16. Wagner C, Barlag B, Gerlach RG, Deiwick J, Hensel M. 2014. The *Salmonella enterica* giant adhesin SiiE binds to polarized epithelial cells in a lectin-like manner. Cell Microbiol 16:962–975. https://doi.org/10.1111/cmi.12253.
17. Gerlach RG, Jackel D, Geymeier N, Hensel M. 2007. Salmonella pathogenicity island 4-mediated adhesion is coregulated with invasion genes in Salmonella enterica. Infect Immun 75:4697–4709. https://doi.org/10.1128/IAI.00228-07.
18. Zhang K, Riba A, Nietschke M, Torow N, Repnik U, Putz A, Fulde M, Dupont A, Hensel M, Hornef M. 2018. Minimal SPI1-T3SS effector requirement for Salmonella enterocyte invasion and intracellular proliferation in vivo. PLoS Pathog 14:e1006925. https://doi.org/10.1371/journal.ppat.1006925.
19. Latasa C, Roux A, Toledo-Arana A, Ghigo J-M, Gamazo C, Penadés JR, Lasa I. 2005. BapA, a large secreted protein required for biofilm formation and host colonization of Salmonella enterica serovar Enteritidis. Mol Microbiol 58:1322–1339. https://doi.org/10.1111/j.1365-2958.2005.04907.x.
20. Yue M, Rankin SC, Blanchet RT, Nulton JD, Edwards RA, Schifferli DM. 2012. Diversification of the Salmonella fimbriae: a model of macro- and microevolution. PLoS One 7:e38596. https://doi.org/10.1371/journal.pone.0038596.
21. Berger CN, Shaw RK, Brown DJ, Mather H, Clare S, Dougan G, Pallen MJ, Frankel G. 2009. Interaction of *Salmonella enterica* with basil and other salad leaves. ISME J 3:261–265. https://doi.org/10.1038/ismej.2008.95.
22. Cui Y, Walcott R, Chen J. 2017. Differential attachment of *Salmonella enterica* and enterohemorrhagic *Escherichia coli* to alfalfa, fenugreek, lettuce, and tomato seeds. Appl Environ Microbiol 83:e03170-16. https://doi.org/10.1128/AEM.03170-16.
23. Hunter PJ, Shaw RK, Berger CN, Frankel G, Pink D, Hand P. 2015. Older leaves of lettuce (*Lactuca* spp.) support higher levels of *Salmonella enterica* ser. Senftenberg attachment and show greater variation between plant accessions than do younger leaves. FEMS Microbiol Lett 362:fnv077.
24. Klerks MM, Franz E, van Gent-Pelzer M, Zijlstra C, van Bruggen AH. 2007. Differential interaction of *Salmonella enterica* serovars with lettuce cultivars and plant-microbe factors influencing the colonization efficiency. ISME J 1:620–631. https://doi.org/10.1038/ismej.2007.82.
25. Kroupitski Y, Golberg D, Belausov E, Pinto R, Swartzberg D, Granot D, Sela S. 2009. Internalization of Salmonella enterica in leaves is induced by light and involves chemotaxis and penetration through open stomata. Appl Environ Microbiol 75:6076–6086. https://doi.org/10.1128/AEM.01084-09.
26. Patel J, Sharma M. 2010. Differences in attachment of Salmonella enterica serovars to cabbage and lettuce leaves. Int J Food Microbiol 139:41–47. https://doi.org/10.1016/j.ijfoodmicro.2010.02.005.
27. Saggers EJ, Waspe CR, Parker ML, Waldron KW, Brocklehurst TF. 2008. Salmonella must be viable in order to attach to the surface of prepared vegetable tissues. J Appl Microbiol 105:1239–1245. https://doi.org/10.1111/j.1365-2672.2008.03795.x.
28. Salazar JK, Deng K, Tortorello ML, Brandl MT, Wang H, Zhang W. 2013. Genes *ycfR*, *sirA* and *yigG* contribute to the surface attachment of *Salmonella enterica* Typhimurium and Saintpaul to fresh produce. PLoS One 8:e57272. https://doi.org/10.1371/journal.pone.0057272.
29. Golberg D, Kroupitski Y, Belausov E, Pinto R, Sela S. 2011. *Salmonella* Typhimurium internalization is variable in leafy vegetables and fresh herbs. Int J Food Microbiol 145:250–257. https://doi.org/10.1016/j.ijfoodmicro.2010.12.031.
30. Kroger C, Dillon SC, Cameron AD, Papenfort K, Sivasankaran SK, Hokamp K, Chao Y, Sittka A, Hebrard M, Handler K, Colgan A, Leekitcharoenphon P, Langridge GC, Lohan AJ, Loftus B, Lucchini S, Ussery DW, Dorman CJ, Thomson NR, Vogel J, Hinton JC. 2012. The transcriptional landscape and small RNAs of *Salmonella enterica* serovar Typhimurium. Proc Natl Acad Sci U S A 109:E1277–E1286. https://doi.org/10.1073/pnas.1201061109.
31. Hansmeier N, Miskiewicz K, Elpers L, Liss V, Hensel M, Sterzenbach T. 2017. Functional expression of the entire adhesiome of *Salmonella enterica* serotype Typhimurium. Sci Rep 7:10326. https://doi.org/10.1038/s41598-017-10598-2.
32. Saini S, Pearl JA, Rao CV. 2009. Role of FimW, FimY, and FimZ in regulating the expression of type I fimbriae in Salmonella enterica serovar Typhimurium. J Bacteriol 191:3003–3010. https://doi.org/10.1128/JB.01694-08.
33. Sterzenbach T, Nguyen KT, Nuccio SP, Winter MG, Vakulskas CA, Clegg S, Romeo T, Bäumler AJ. 2013. A novel CsrA titration mechanism regulates fimbrial gene expression in Salmonella typhimurium. EMBO J 32:2872–2883. https://doi.org/10.1038/emboj.2013.206.
34. Barnhart MM, Chapman MR. 2006. Curli biogenesis and function. Annu Rev Microbiol 60:131–147. https://doi.org/10.1146/annurev.micro.60.080805.142106.
35. Main-Hester KL, Colpitts KM, Thomas GA, Fang FC, Libby SJ. 2008. Coordinate regulation of Salmonella pathogenicity island 1 (SPI1) and SPI4 in Salmonella enterica serovar Typhimurium. Infect Immun 76:1024–1035. https://doi.org/10.1128/IAI.01224-07.
36. Kingsley RA, Santos RL, Keestra AM, Adams LG, Bäumler AJ. 2002. Salmonella enterica serotype Typhimurium ShdA is an outer membrane fibronectin-binding protein that is expressed in the intestine. Mol Microbiol 43:895–905. https://doi.org/10.1046/j.1365-2958.2002.02805.x.
37. Dorsey CW, Laarakker MC, Humphries AD, Weening EH, Bäumler AJ. 2005. *Salmonella enterica* serotype Typhimurium MisL is an intestinal

colonization factor that binds fibronectin. Mol Microbiol 57:196–211. https://doi.org/10.1111/j.1365-2958.2005.04666.x.
38. Raghunathan D, Wells TJ, Morris FC, Shaw RK, Bobat S, Peters SE, Paterson GK, Jensen KT, Leyton DL, Blair JM, Browning DF, Pravin J, Flores-Langarica A, Hitchcock JR, Moraes CT, Piazza RM, Maskell DJ, Webber MA, May RC, MacLennan CA, Piddock LJ, Cunningham AF, Henderson IR. 2011. SadA, a trimeric autotransporter from Salmonella enterica serovar Typhimurium, can promote biofilm formation and provides limited protection against infection. Infect Immun 79:4342–4352. https://doi.org/10.1128/IAI.05592-11.
39. Lambert MA, Smith SG. 2009. The PagN protein mediates invasion via interaction with proteoglycan. FEMS Microbiol Lett 297:209–216. https://doi.org/10.1111/j.1574-6968.2009.01666.x.
40. Rosselin M, Virlogeux-Payant I, Roy C, Bottreau E, Sizaret PY, Mijouin L, Germon P, Caron E, Velge P, Wiedemann A. 2010. Rck of Salmonella enterica, subspecies enterica serovar enteritidis, mediates zipper-like internalization. Cell Res 20:647–664. https://doi.org/10.1038/cr.2010.45.
41. Tan MS, White AP, Rahman S, Dykes GA. 2016. Role of fimbriae, flagella and cellulose on the attachment of Salmonella Typhimurium ATCC 14028 to plant cell wall models. PLoS One 11:e0158311. https://doi.org/10.1371/journal.pone.0158311.
42. Rossez Y, Holmes A, Wolfson EB, Gally DL, Mahajan A, Pedersen HL, Willats WG, Toth IK, Holden NJ. 2014. Flagella interact with ionic plant lipids to mediate adherence of pathogenic Escherichia coli to fresh produce plants. Environ Microbiol 16:2181–2195. https://doi.org/10.1111/1462-2920.12315.
43. Kutschera A, Ranf S. 2019. The multifaceted functions of lipopolysaccharide in plant-bacteria interactions. Biochimie 159:93–98. https://doi.org/10.1016/j.biochi.2018.07.028.
44. Iniguez AL, Dong Y, Carter HD, Ahmer BM, Stone JM, Triplett EW. 2005. Regulation of enteric endophytic bacterial colonization by plant defenses. Mol Plant Microbe Interact 18:169–178. https://doi.org/10.1094/MPMI-18-0169.
45. Garcia AV, Charrier A, Schikora A, Bigeard J, Pateyron S, de Tauzia-Moreau ML, Evrard A, Mithofer A, Martin-Magniette ML, Virlogeux-Payant I, Hirt H. 2014. Salmonella enterica flagellin is recognized via FLS2 and activates PAMP-triggered immunity in Arabidopsis thaliana. Mol Plant 7:657–674. https://doi.org/10.1093/mp/sst145.
46. Hölzer SU, Schlumberger MC, Jäckel D, Hensel M. 2009. Effect of the O-antigen length of lipopolysaccharide on the functions of type III secretion systems in *Salmonella enterica*. Infect Immun 77:5458–5470. https://doi.org/10.1128/IAI.00871-09.
47. Jang H, Matthews KR. 2018. Influence of surface polysaccharides of *Escherichia coli* O157:H7 on plant defense response and survival of the human enteric pathogen on *Arabidopsis thaliana* and lettuce (*Lactuca sativa*). Food Microbiol 70:254–261. https://doi.org/10.1016/j.fm.2017.10.013.
48. Balsanelli E, Serrato RV, de Baura VA, Sassaki G, Yates MG, Rigo LU, Pedrosa FO, de Souza EM, Monteiro RA. 2010. *Herbaspirillum seropedicae rfbB* and *rfbC* genes are required for maize colonization. Environ Microbiol 12:2233–2244. https://doi.org/10.1111/j.1462-2920.2010.02187.x.
49. Salih O, Remaut H, Waksman G, Orlova EV. 2008. Structural analysis of the Saf pilus by electron microscopy and image processing. J Mol Biol 379:174–187. https://doi.org/10.1016/j.jmb.2008.03.056.
50. Hung DL, Knight SD, Woods RM, Pinkner JS, Hultgren SJ. 1996. Molecular basis of two subfamilies of immunoglobulin-like chaperones. EMBO J 15:3792–3805. https://doi.org/10.1002/j.1460-2075.1996.tb00753.x.
51. Zeng L, Zhang L, Wang P, Meng G. 2017. Structural basis of host recognition and biofilm formation by Salmonella Saf pili. Elife 6:e28619. https://doi.org/10.7554/eLife.28619.
52. Laniewski P, Baek CH, Roland KL, Curtiss R, 3rd. 2017. Analysis of spleen-induced fimbria production in recombinant attenuated *Salmonella enterica* serovar Typhimurium vaccine strains. mBio 8:e01189-17. https://doi.org/10.1128/mBio.01189-17.
53. Chessa D, Dorsey CW, Winter M, Bäumler AJ. 2008. Binding specificity of *Salmonella* plasmid-encoded fimbriae assessed by glycomics. J Biol Chem 283:8118–8124. https://doi.org/10.1074/jbc.M710095200.
54. Jonas K, Tomenius H, Kader A, Normark S, Römling U, Belova LM, Melefors O. 2007. Roles of curli, cellulose and BapA in *Salmonella* biofilm morphology studied by atomic force microscopy. BMC Microbiol 7:70. https://doi.org/10.1186/1471-2180-7-70.
55. Guttula D, Yao M, Baker K, Yang L, Goult BT, Doyle PS, Yan J. 2019. Calcium-mediated protein folding and stabilization of *Salmonella* biofilm-associated protein A. J Mol Biol 431:433–443. https://doi.org/10.1016/j.jmb.2018.11.014.
56. Lawes M, Maloy S. 1995. Mu*dSacI*, a transposon with strong selectable and counterselectable markers: use for rapid mapping of chromosomal mutations in *Salmonella typhimurium*. J Bacteriol 177:1383–1387. https://doi.org/10.1128/jb.177.5.1383-1387.1995.
57. Kang HY, Dozois CM, Tinge SA, Lee TH, Curtiss R, III. 2002. Transduction-mediated transfer of unmarked deletion and point mutations through use of counterselectable suicide vectors. J Bacteriol 184:307–312. https://doi.org/10.1128/jb.184.1.307-312.2002.
58. Datsenko KA, Wanner BL. 2000. One-step inactivation of chromosomal genes in Escherichia coli K-12 using PCR products. Proc Natl Acad Sci U S A 97:6640–6645. https://doi.org/10.1073/pnas.120163297.
59. Hoffmann S, Schmidt C, Walter S, Bender JK, Gerlach RG. 2017. Scarless deletion of up to seven methyl-accepting chemotaxis genes with an optimized method highlights key function of CheM in *Salmonella* Typhimurium. PLoS One 12:e0172630. https://doi.org/10.1371/journal.pone.0172630.
60. Herrero M, de Lorenzo V, Timmis KN. 1990. Transposon vectors containing non-antibiotic resistance selection markers for cloning and stable chromosomal insertion of foreign genes in gram-negative bacteria. J Bacteriol 172:6557–6567. https://doi.org/10.1128/jb.172.11.6557-6567.1990.
61. Woodcock DM, Crowther PJ, Doherty J, Jefferson S, DeCruz E, Noyer-Weidner M, Smith SS, Michael MZ, Graham MW. 1989. Quantitative evaluation of Escherichia coli host strains for tolerance to cytosine methylation in plasmid and phage recombinants. Nucleic Acids Res 17:3469–3478. https://doi.org/10.1093/nar/17.9.3469.
62. Simon R, Priefer U, Pühler A. 1983. A broad host range mobilization system for in vivo genetic engineering: transposon mutagenesis in Gram negative bacteria. Nat Biotechnol 1:784–791. https://doi.org/10.1038/nbt1183-784.
63. Stojiljkovic I, Bäumler AJ, Heffron F. 1995. Ethanolamine utilization in Salmonella typhimurium: nucleotide sequence, protein expression, and mutational analysis of the cchA cchB eutE eutJ eutG eutH gene cluster. J Bacteriol 177:1357–1366. https://doi.org/10.1128/jb.177.5.1357-1366.1995.
64. Lilleengen L. 1948. Typing *Salmonella typhimurium* by means of bacteriophage. Acta Pathol Microbiol Scand Suppl 77:11–125. https://doi.org/10.1111/j.1699-0463.1952.tb00174.x.
65. Schneider HA, Zinder ND. 1956. Nutrition of the host and natural resistance to infection. V. An improved assay employing genetic markers in the double strain inoculation test. J Exp Med 103:207–223. https://doi.org/10.1084/jem.103.2.207.
66. Weening EH, Barker JD, Laarakker MC, Humphries AD, Tsolis RM, Bäumler AJ. 2005. The *Salmonella enterica* serotype Typhimurium *lpf*, *bcf*, *stb*, *stc*, *std*, and *sth* fimbrial operons are required for intestinal persistence in mice. Infect Immun 73:3358–3366. https://doi.org/10.1128/IAI.73.6.3358-3366.2005.
67. Grin I, Hartmann MD, Sauer G, Hernandez Alvarez B, Schutz M, Wagner S, Madlung J, Macek B, Felipe-Lopez A, Hensel M, Lupas A, Linke D. 2014. A trimeric lipoprotein assists in trimeric autotransporter biogenesis in enterobacteria. J Biol Chem 289:7388–7398. https://doi.org/10.1074/jbc.M113.513275.
68. Gerlach RG, Claudio N, Rohde M, Jäckel D, Wagner C, Hensel M. 2008. Cooperation of Salmonella pathogenicity islands 1 and 4 is required to breach epithelial barriers. Cell Microbiol 10:2364–2376. https://doi.org/10.1111/j.1462-5822.2008.01218.x.
69. Zenk SF, Jantsch J, Hensel M. 2009. Role of Salmonella enterica lipopolysaccharide in activation of dendritic cell functions and bacterial containment. J Immunol 183:2697–2707. https://doi.org/10.4049/jimmunol.0900937.
70. Krieger V, Liebl D, Zhang Y, Rajashekar R, Chlanda P, Giesker K, Chikkaballi D, Hensel M. 2014. Reorganization of the endosomal system in *Salmonella*-infected cells: the ultrastructure of *Salmonella*-induced tubular compartments. PLoS Pathog 10:e1004374. https://doi.org/10.1371/journal.ppat.1004374.
71. Lorkowski M, Felipe-Lopez A, Danzer CA, Hansmeier N, Hensel M. 2014. *Salmonella enterica* invasion of polarized epithelial cells is a highly cooperative effort. Infect Immun 82:2657–2667. https://doi.org/10.1128/IAI.00023-14.
72. Fulde M, Sommer F, Chassaing B, van Vorst K, Dupont A, Hensel M, Basic M, Klopfleisch R, Rosenstiel P, Bleich A, Backhed F, Gewirtz AT, Hornef MW. 2018. Neonatal selection by Toll-like receptor 5 influences long-term gut microbiota composition. Nature 560:489–493. https://doi.org/10.1038/s41586-018-0395-5.

73. Wille T, Wagner C, Mittelstadt W, Blank K, Sommer E, Malengo G, Döhler D, Lange A, Sourjik V, Hensel M, Gerlach RG. 2014. SiiA and SiiB are novel type I secretion system subunits controlling SPI4-mediated adhesion of *Salmonella enterica*. Cell Microbiol 16:161–178. https://doi.org/10.1111/cmi.12222.
74. St-Pierre F, Cui L, Priest DG, Endy D, Dodd IB, Shearwin KE. 2013. One-step cloning and chromosomal integration of DNA. ACS Synth Biol 2:537–541. https://doi.org/10.1021/sb400021j.
75. Alting-Mees MA, Short JM. 1989. pBluescript II: gene mapping vectors. Nucleic Acids Res 17:9494. https://doi.org/10.1093/nar/17.22.9494.
76. Raffatellu M, George MD, Akiyama Y, Hornsby MJ, Nuccio SP, Paixao TA, Butler BP, Chu H, Santos RL, Berger T, Mak TW, Tsolis RM, Bevins CL, Solnick JV, Dandekar S, Bäumler AJ. 2009. Lipocalin-2 resistance confers an advantage to *Salmonella enterica* serotype Typhimurium for growth and survival in the inflamed intestine. Cell Host Microbe 5:476–486. https://doi.org/10.1016/j.chom.2009.03.011.
77. Kingsley RA, Reissbrodt R, Rabsch W, Ketley JM, Tsolis RM, Everest P, Dougan G, Bäumler AJ, Roberts M, Williams PH. 1999. Ferrioxamine-mediated iron(III) utilization by *Salmonella enterica*. Appl Environ Microbiol 65:1610–1618. https://doi.org/10.1128/AEM.65.4.1610-1618.1999.